Archaeological Discovery, 2025, 13(3), 115-152
https://www.scirp.org/journal/ad
ISSN Online: 2331-1967
ISSN Print: 2331-1959

White Particles on the Turin Shroud: Optical Microscopy Studies and SEM-EDX Analyses

Gérard Lucotte[1*], Thierry Thomasset[2], Stéphan Borensztajn[3]

[1]Institute of Molecular Anthropology, Paris, France
[2]Laboratory of Physico-Chemical Analysis, UST de Compiègne, Compiègne, France
[3]Institute of Physics of the Globe, Paris, France
Email: *lucottegerard@outlook.fr

How to cite this paper: Lucotte, G., Thomasset, T., & Borensztajn, S. (2025). White Particles on the Turin Shroud: Optical Microscopy Studies and SEM-EDX Analyses. *Archaeological Discovery, 13,* 115-152.
https://doi.org/10.4236/ad.2025.133007

Received: April 14, 2025
Accepted: June 23, 2025
Published: June 26, 2025

Abstract

We have explored by optical microscopy and scanning electron microscopy coupled with energy dispersive X-ray about one hundred and fifty particles of white pigments located in a sample of the Face area of the Turin Shroud. Twenty-one of them are micro-fragments of marble. Thirty-two of them are particles of different Coccolith species of chalk. More than fifty of them are ceruse micro-plaques and four are ceruse plaques (yellow in colour); about sixty-four are ceruse micro-balls. The white of zinc is represented by only one particle. There is one paint film of titanium dioxide and nine other micro-plaques, micro-scales and micro-balls of this pigment. All these particles contribute significantly to the bleaching of the Turin Shroud.

Keywords

Turin Shroud, Face Area, White Pigments, Marble, Coccoliths, Ceruse, White of Zinc, Titanium Dioxide, Optical Microscopy, Scanning Electron Microscopy, Energy Dispersive X-Ray

1. Introduction

The Turin Shroud (TS), the most important Christ's relic, is a well-known object in which a body image is imprinted (Marion & Lucotte, 2006). We have obtained a small triangular sticky tape that was sampled on its surface (corresponding to the Face of this body) and we concentrated in the past years on the study of microscopic particles located on the surface of this sticky tape (Lucotte, 2017). More recently we published gold and silver particles (Lucotte, 2022), some peculiar little clays (Lucotte, 2023), lapis lazuli particles (Lucotte & Thomasset, 2023), some little micro-organisms having chemical formulas similar to those of clays (Lucotte,

2024) iron-rich red clays (Lucotte et al., 2024) and brass particles (Lucotte & Thomasset, 2024) detected on the surface of the triangle.

In the present study we described in details, by optic microscopy and SEM-EDX analyses, all the particles of white pigments (mineral and metallic) that we found on the triangle surface.

2. Material and Methods

The material is the small (1.36 mm height, 614 µm wide) sticky tape triangle at the surface of which all particles were deposited. For practical reasons, the surface of this triangle was subdivided into nineteen sub-samples areas, named A to S; because of its complexity, the F area was subdivided into seven (a to g) sub-areas (Lucotte, 2017).

The samples of references used are: a powder of marble ("poudre de marbre", Dugay, Saint Ouen, France); a white of chalk ("baton de craie"); a ceruse ("blanc d'argent", Sennelier, Paris); a white of zinc ("blanc de zinc", Corector, Paris); a lithopone powder ("blanc de lithophone" Sennelier); a zinc sulphate ("sulphate de zinc heptahydraté", Coopération Pharmaceutique Française, Melun, France); a white of titanium ("blanc de titane", Dugay).

All the particles of white pigments were observed (to determinate colour) by optical microscopy (both in direct and inverted positions of the triangle), using a photo-microscope Zeiss (model III, 1972).

These particles were also observed, with any preparation, on the adherent part of the surface of the triangle. These observations were first conducted by SEM (Scanning Electron Microscopy), using a Philips XL Instrument (of the environmental version). GSE (Gazeous Secondary Electrons) and BSE (Back Scattered Electrons) procedures were used, the second one to better detect heavy elements. Elemental analyses for each particle observed were realized by EDX (Energy Dispersive X-ray), this SEM microscope being equipped with a Bruker probe AXS-EDX (the system analysis is PGT: Spirit Model of Princeton Gamma Technology).

Particles m39 and m41 were examined with another SEM apparatus (SEM2): a FEI model Quanta 25 of FEG, both in LFD (Large Field Detector) and CBS (Circular Back Scattering) procedures.

Almost all of the white pigments of reference were studied by a third SEM apparatus (SEM3), an Auriga FEG-FIB (Zeiss), images being performed in secondary electrons (SE).

Each elemental analysis is given in the form of a spectrum, with kiloelectrons/Volts (ke/V) on the abscissa and elemental peak heights in ordinates. Highly Resolutive (HR) spectra are those where the ordinate graduations are enhanced, to better see element peaks.

3. Results

White pigments studied here are mineral (white of marble and white of chalk) or metallic (white of lead, whites of zinc and white of titanium). All are whites that were used in painting, at different periods of time.

3.1. White of Marble

Lime white ($CaCO_3$) is the oldest white pigment in the world. It was probably used as white pigment as its more compact form, that of a "dense" calcium carbonate (that with an elevated main calcium peak, like that of marble). Today marble powder is again used, mainly to paint in white stucco paints and plasters.

Figure 1 summarizes results obtained concerning a commercial marble powder of reference. The SEM photograph of the figure shows that it is constituted of grains, the more little ones (between 5 and 20 μm of maximal dimensions) being elongated with angulous outlines. The global spectrum of this powder is that of a dense calcium carbonate.

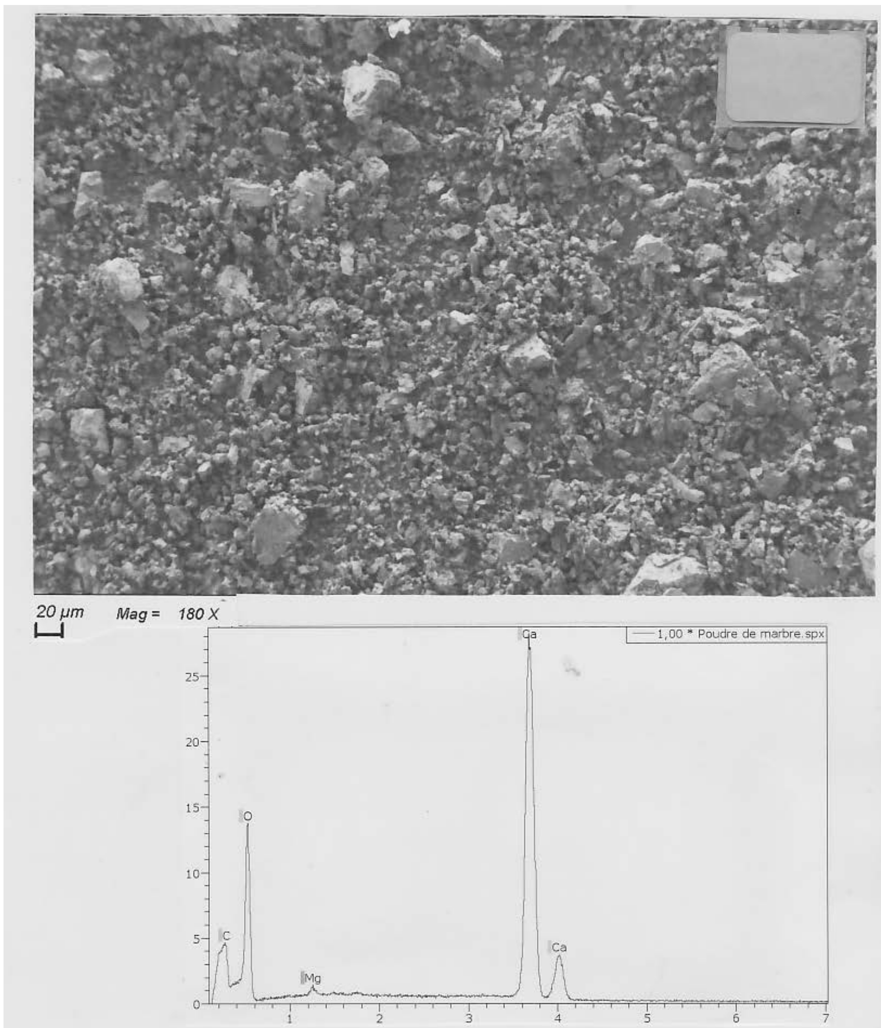

Figure 1. The powder of marble of reference. *Above*: SEM3 photograph (180×) of this powder; insert shows the white colour of this powder. *Below*: Global spectrum of the powder. C: carbon; O: oxygen; Mg (traces): magnesium; Ca (two peaks): calcium.

There are twenty-one particles of marble located in the various areas of the triangle. As an example, **Figure 2** summarizes results obtained concerning particle a34, located in area A of the triangle. Photograph of that figure shows neighbouring particles of a34: a33, a pollen (Lucotte, 2015); a40, a colouring pigment; a41, a calcium phosphate iron-rich; a42, a glass fragment; a43, a trilobate calcium carbonate. The a34 particle is elongated and of about 10 µm of maximal size. Its spectrum is that of a dense calcium carbonate, the main Ca (calcium) peak being almost as elevated as that of the carbon (C); in the spectrum, there are traces of Mg (magnesium), Al (aluminium), Si (silicium) and chlorine (Cl). Its colour is white in optic microscopy.

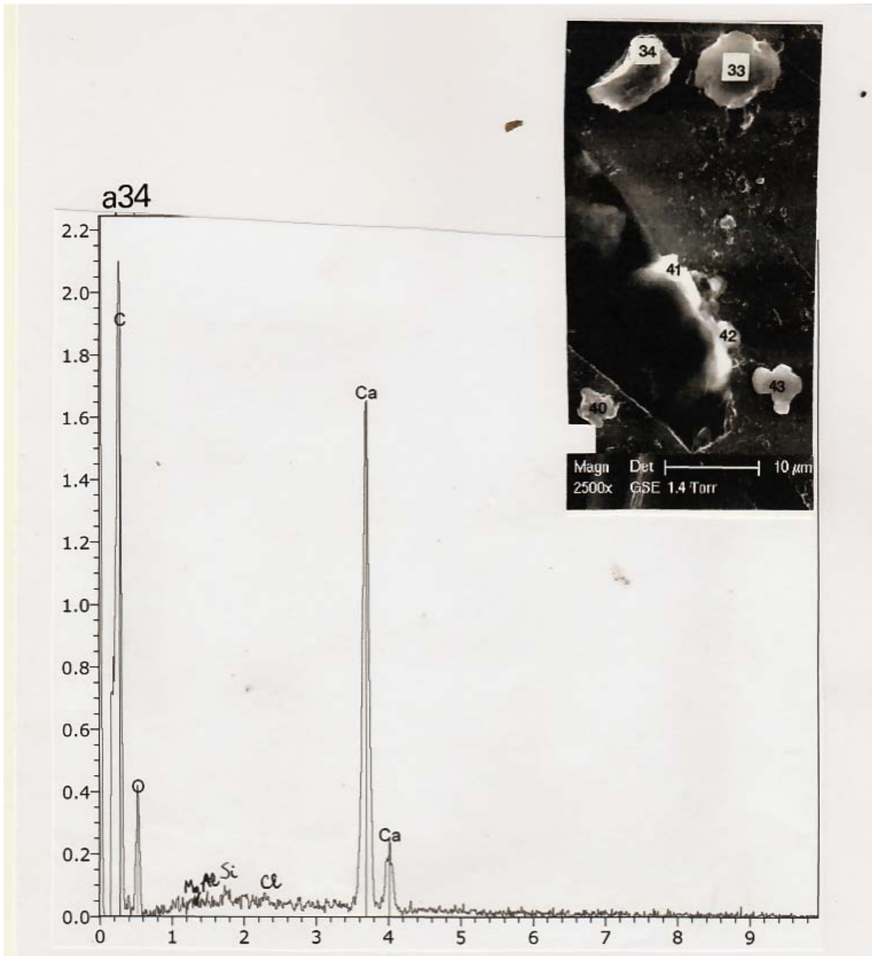

Figure 2. The a34 marble particle. *Above*: SEM1 photograph (2500×), in GSE, of the left lower part of the A area showing the a34 particle. *Below*: The HD spectrum of a34. C: carbon; O: oxygen; Mg (traces): magnesium; Al (traces): aluminium; Si (traces): silicium; Cl (traces): chlorine; Ca (two peaks): calcium.

There are one marble particle in the B area (b78-1), one in the E.c area (e54), two in the F area (f39 and f40), three in the H area (h31, h45 and h52), one in the I area (i40), four in the J area (j11, j22, j49 and j55), three in the K area (k45, k47 and k62), one in the P area (p7), three in the Q area (q3, q10 and q13) and one in the R area (r14).

Table 1 gives the list and characterizations of the twenty-one detected particles of marble. Their forms are generally elongated, with angular outlines and their approximate maximal lengths are between 3 and 19 µm. Their spectra are typic of dense calcium carbonate; all of them contains silicium as a minor peak.

Table 1. List and characteristics of the twenty-one particles of marble located in the areas of the triangle.

Particles	Areas	Nomenclature	Forms	Maximal lengths (in µm)	Typical Spectra	Si	Colours	Peculiarities
1	A	a34	elongated	12	+	traces	white	
2	B	b78-1	acutiform	4	+	+	white	on the lower border of b78
3	E.c	e54	rectangular	4.5	+	+	white	
4	F	f39	acutiform	3	+	+	white	
5	F	f40	rectangular	5	+	+	white	
6	H	h31	elongated	8.5	+	+	white	
7	H	h45	triangular	3.5	+	+	white	
8	H	h52	triangular	3.5	+	+	white	
9	I	i40	hexagonal	6.5	+	+	white	
10	J	j11	elongated	3.5	+	traces	white	
11	J	j22	elongated	9.5	+	traces	white	
12	J	j49	squared	7.5	+	+	not visible	with Ti and Fe
13	J	j55	elongated	13.5	+	+	not visible	
14	K	k45	elongated	8	+	+	white	
15	K	k47	elongated	7.5	+	+	white	
16	K	k62	triangular	19	+	traces	white	striated longitudinally
17	P	p7	elongated	7.5	+	+	white	
18	Q	q3	elongated	8.5	+	traces	white	
19	Q	q10	triangular	6	+	+	white	
20	Q	q13	elongated	4.5	+	traces	not visible	
21	R	r14	elongated	9.5	+	+	white	

Colours (not visible for particles j49, j55 and q13, because of their proximities to the triangle border) are white in optic microscopy.

3.2. White of Chalk

Chalk is a very pure limestone, formed during the Cretaceous period, of fine calcite crystals consisting mainly of fossil remains of the shells and skeletons of microscopic plankton, that of Haptophytes (Coccoliths).

Figure 3 summarizes results obtained concerning a commercial chalk powder of reference. This powder is white, being constituted of small particles (of 5 µm of sizes). The global spectrum of this powder is mainly that of a calcium carbonate (with a very elevated main peak of calcium). Figure 4 shows a Coccolith of this powder; it is round in form and of about 5 µm of diameter. It is constituted of numerous micro-plaques, alternating at its outline. Other particles of the photograph correspond mainly to dissociated plaques of other Coccoliths.

Figure 3. The chalk powder of reference. *Above*: SEM3 photographs (30×), in CBS, of the chalk powder; insert: the chalk powder in optic microscopy. *Below*: Global spectrum of the chalk powder. C: carbon; O: oxygen; Si (traces): silicium; Ca (two peaks): calcium.

Most of the Coccoliths found on the triangle surface are incomplete, consisting of a little number of chipboard or separated plaques. When complete, it is evident that they belong to different genders and species of Coccoliths. For some of them that are complete we have attempted to determinate genders from which they belong according to their appearances, comparing to those already published (Heimdal, 1993).

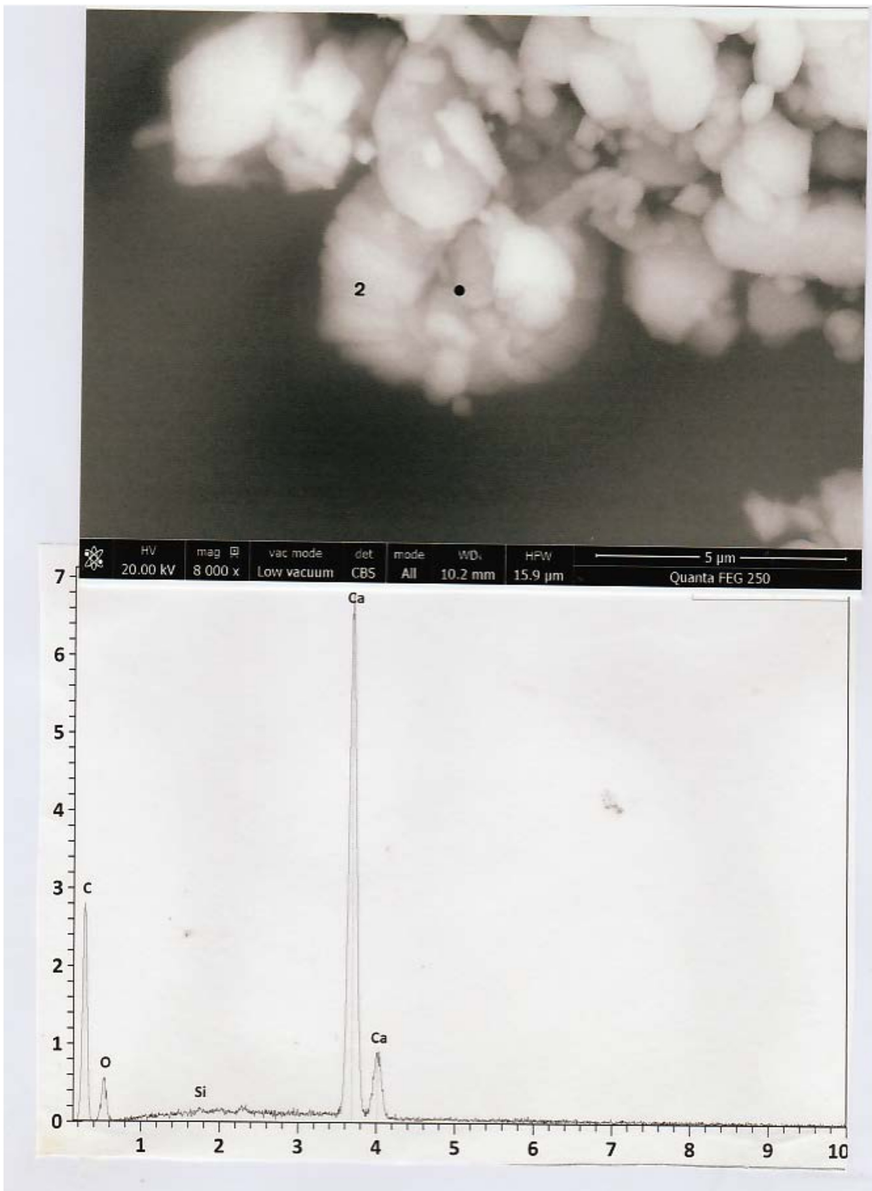

Figure 4. Aspect and spectrum of a Coccolith of the chalk powder. *Above*: SEM2 photograph (8000×), in CBS, of the Coccolith; the black spot indicates the approximate location where the SEM-EDX analysis was realized. *Below*: The Coccolith spectrum. C: carbon; O: oxygen; Si (traces): silicium; Ca (two peaks): calcium.

There are two Coccoliths in the A area: a10 and a36-36'. The a10 particle, located near the left border of the upper part of the A area, is a formation of at least four Coccolith plaques of about 4 µm of maximal size. The a36-36' particle, located near the left border below the previous, is a complete Coccolith (Figure 5) of an oval form and size of about 9.5 µm. At least twenty external plaques are visible inside a36-36', some of them (in the apex) being stomated. We assimilate this Coccolith to the gender **Acanthoica**.

There are three Coccoliths in the B area: b50, b67, and b74'. The b50 formation is in fact a set of at least nine separated Coccolith plaques, covering a total surface of 19 μm, located in the right part of the B area between particles b44 (a rounded carbonate), b51 (a squared carbonate), b53 (an aluminium piece), b52 (a ceramic fragment) and b49 and b49' (two quartz particles). The b67 particle, located near the left border of the B area, is a trilobed Coccolith of 9 μm formed of five plaques.

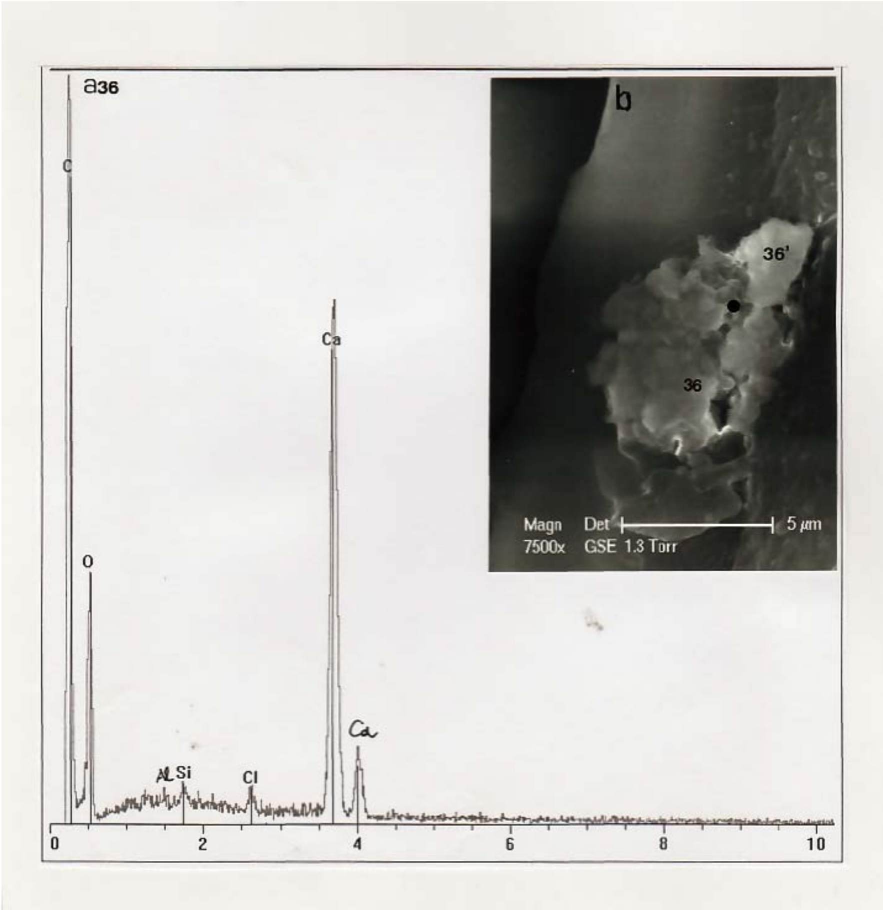

Figure 5. The a36-36' Coccolith. *Above*: SEM1 photograph (7500×), in GSE, of some part of the left border of the A area showing a36-36' (b indicates the left border of the triangle). *Below*: The a36 spectrum. C: carbon; O: oxygen; Al (traces): aluminium; Si: silicium; Cl: chlorine; Ca (two peaks): calcium.

The b74' particle (Figure 6), located near the left extremity of the b74 particle—which is an iron-rich clay (Lucotte et al., 2024)—in the lower part of the B area, is a composite plaque located above a set of seven minor plaques, the whole constituting an oval Coccolith of 6.5 μm.

There are two Coccoliths in the D area: d30 and d34. The d30 particle (Figure 7), located in the left part of the D area, is a rounded Coccolith of 6 μm of diameter formed of six plaques plus two additional plaques at the periphery. We assimilate its to the gender **Sphaerocalyptra**.

The d34 particle is a very eroded Coccolith, located in the lower left part of the D area, is of 9.5 μm of size (where seven plaques can be discerned).

There are two Coccoliths in the E area: e3 and e114. The e3 Coccolith, located on the top of the E.a area, is cupuliform, of 8 μm and formed of seven plaques (**Figure 8**). We assimilate its to the gender **Oolithus**. The e114 Coccolith, located in the E.e area, is pentalobed; its size is of 8 μm and it is formed of at least six plaques.

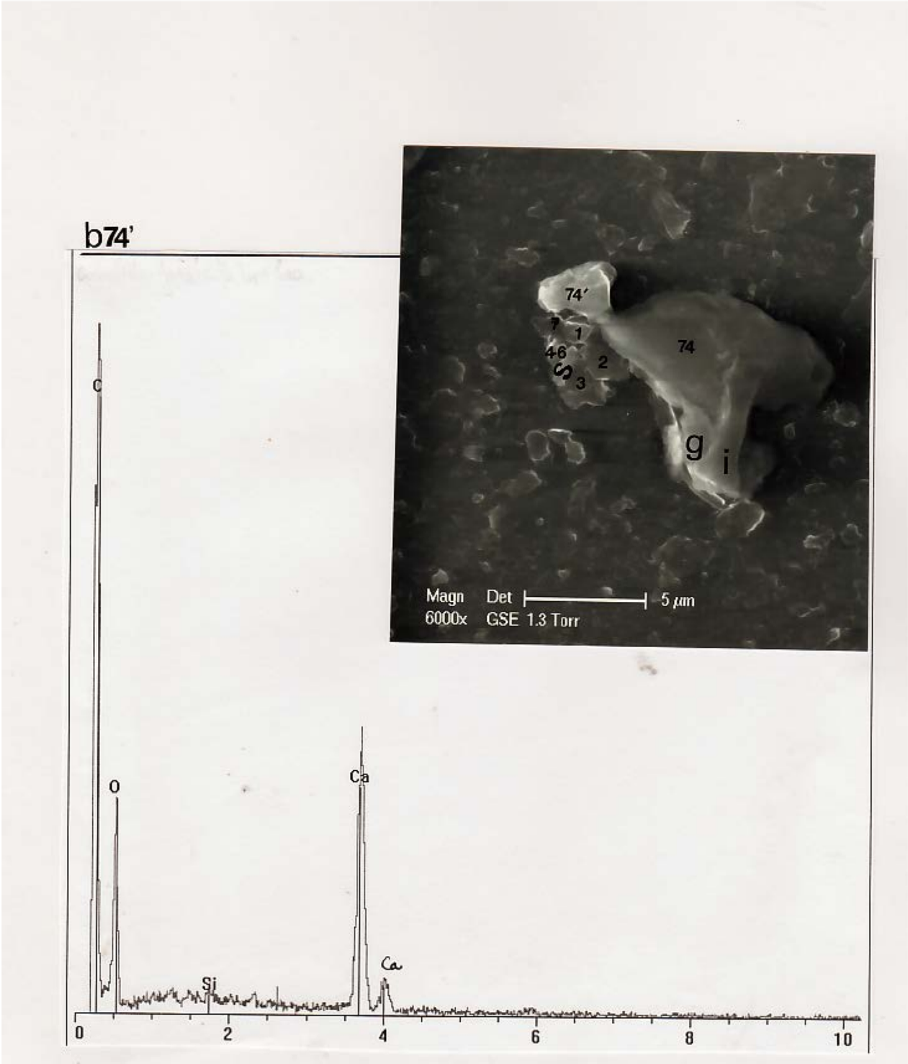

Figure 6. The Coccolith b74' - 1-7. *Above*: SEM1 photograph (6000×), in GSE, of the b74' - 1-7 particles, located in the lower part of the B area (S: a gypsum stick; i: an iron stick; g: an Ostracod; b74: an iron-rich clay). Below: The b74' - 1-7 spectrum.

There are two Coccoliths in the F area: f1 and f3, both located in the superior part of the area. The f1 Coccolith is cupuliform, and of 7.5 μm of length; seven plaques are visible in its superior part. The f3 Coccolith, very eroded, is oval and of 6 μm; more than twenty micro-plaques are visible on one of its side.

The particle h19 is the only Coccolith found in the H area (it is located at the top of the Diatom h20). The h19 Coccolith is elongated, with at least seven visible external plaques.

There are five Coccoliths in the I area: i5, i6 and i30 in its lateral right part and i48 and i56 in its lower part. The i5 Coccolith is trilobed, of 8.5 μm and contains about sixteen micro-plaques. The i6 Coccolith is pentagonal, of 7 μm and contains eight micro-plaques. The i30 Coccolith is rounded, of 4.5 μm and contains three micro-plaques. The i48 Coccolith is pentalobed, of 10 μm and contains six micro-plaques.

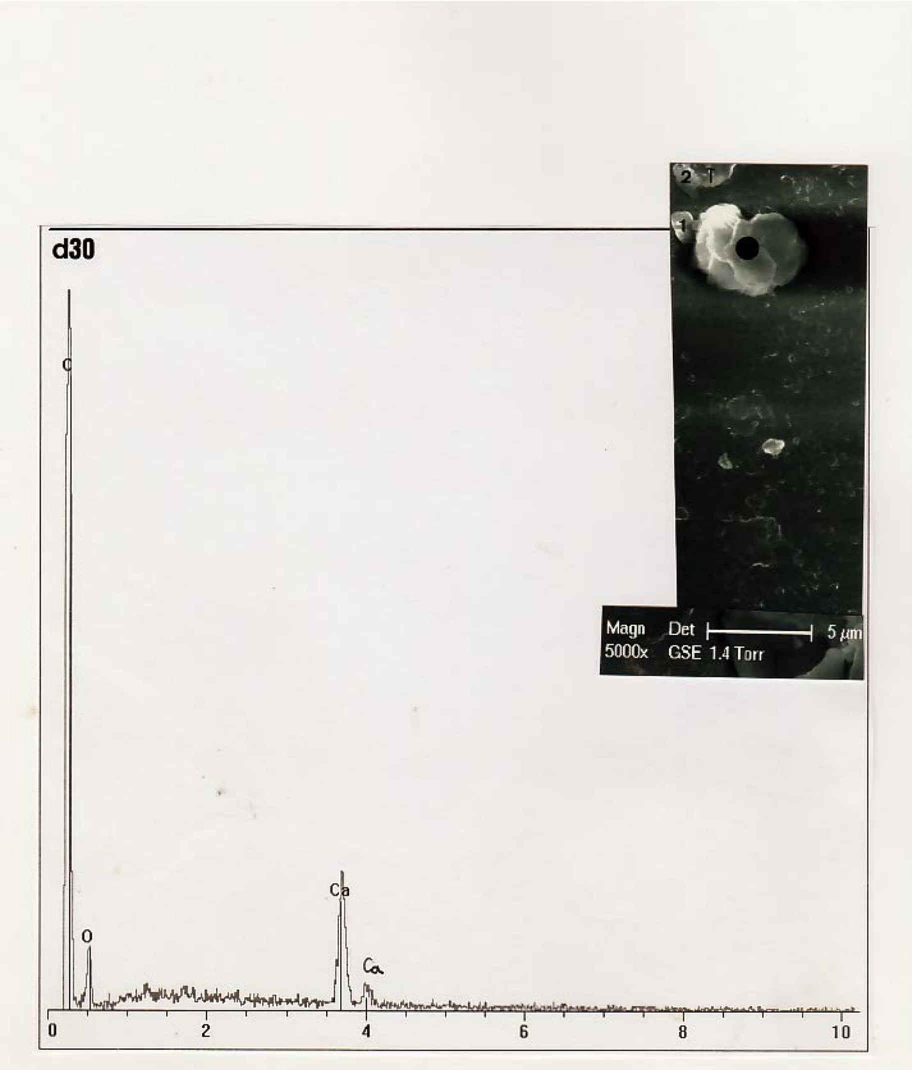

Figure 7. The d30 Coccolith. *Above*: SEM1 photograph (5000×), in GSE, of the left lower part of the D area showing d30 (1,2: detached plaques from d30; T: hole). *Below*: The d30 spectrum.

Photograph of **Figure 9** shows the i56 Coccolith and its neighbouring particles: i57 is a painting fragment with silver (Lucotte, 2022) and barium sulphate (i56') at its other extremity; i55 is a lapis-lazuli (Lucotte & Thomasset, 2023). The i56 Coccolith is trilobed, of 5 μm and contains twelve micro-plaques.

The j65 Coccolith (**Figure 10**) is located in the left lower part of the J area. It is oval, of 9.5 μm and contains more than twenty micro-plaques.

There are two Coccoliths in the K area: k3-4-5 and k 51. Photograph of **Figure 11** shows some part of the K area with k3-4-5. Other neighbouring particles in that area are: k1, a brass (Lucotte & Thomasset, 2024); k2, a barium sulphate; k6, a PVC plastic; k7, a lapis-lazuli; k8, a calcite; k10, a fiber; k11, a Cyanophycae; k12, a Dinophycae; k13, a brass; k14, an organic particle. The k3-4-5 Coccolith is oval and of 10.5 µm; it contains seven micro-plaques, whose three are voluminous (about 3 µm of dimensions) and rounded. We assimilate the k3-4-5 Coccolith to the gender **Discolithina.**

Figure 8. The e3 Coccolith. *Above*: SEM photograph (12,500×), in GSE, of e3, located in some part of the E.a area (1 - 7: the seven plaques). *Below*: The e3 spectrum.

The photograph of Figure 12 shows some lower part of the K area with the k51 Coccolith. Other neighbouring particles in that area are: k51 and k52 two silices; k54, a painting fragment containing barium sulphate; k55, a PVC plastic. The k51 Coccolith is ovoïd, of 4.5 µm and contains six plaques.

There are three Coccoliths in the L area: l46, l51-52-53 and l65. Photograph of Figure 13 shows, in the middle part of the L area, the l46 Coccolith. It is quadrilobed, of 5.5 µm and formed of at least fifteen plaques. We assimilate it to the gender **Florisphaera**.

The l51-52-53 Coccolith is located in the left lower part of the L area. It is oval and of 8 µm; it is formed of six micro-plaques, plus two exterior plaques (l52 and l53).

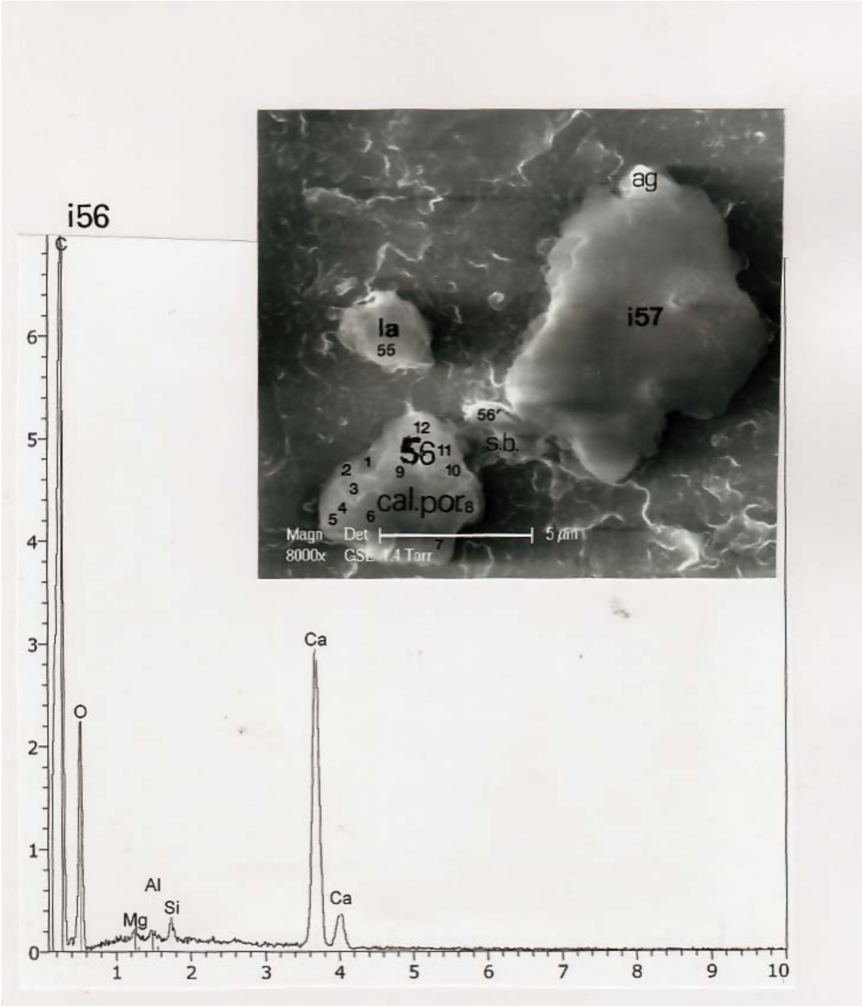

Figure 9. The i56 Coccolith. *Above*: SEM1 photograph (8000×), in GSE, of some lower part of the I area showing i56 (Ag: silver; s.b. barium sulphate; la: lapis lazuli). The twelve (1 - 12) micro-plaques inside of the i56 particle (por. cal.: porous calcite) are indicated. *Below*: The i56 spectrum.

Photograph of Figure 14 shows, in the right part of the L area, the l65 Coccolith. It had a form of an urn; its size is of 7.5 µm and it is formed of more than seven micro-plaques. We assimilate it to the gender **Daktylethra**.

There are three Coccoliths in the M area: m13, m40 and m43. The m13 Coccolith is located in the left part of the M area. It is quadrilobed, of 6.5 µm and formed of six plaques. The m40 and m43 Coccoliths are located in the right part of the M area. The m40 Coccolith is triangular, of 8 µm and formed of at least seven micro-plaques. The m43 Coccolith is pentalobed, of 9.5 µm and formed of at least twelve micro-plaques.

The q8 Coccolith, located in the upper right part of the Q area, is oval, of 2.5 µm and formed of at least eight micro-plaques.

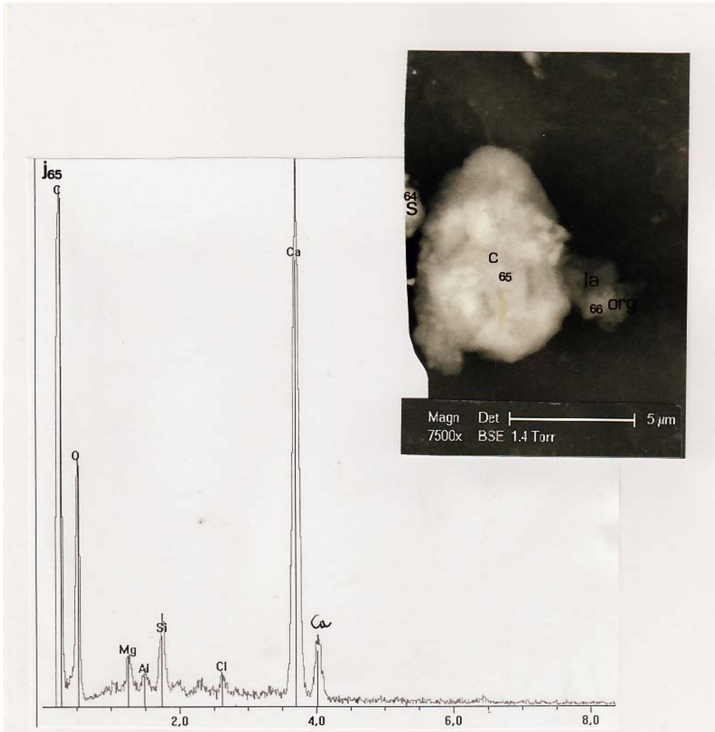

Figure 10. The j65 Coccolith. *Above*: SEM1 photograph (7500×) of some part of the J area (in BSE) showing j65 (c: Coccolith; or: organic; la: lapis lazuli; S: Diatom). *Below*: The j65 spectrum.

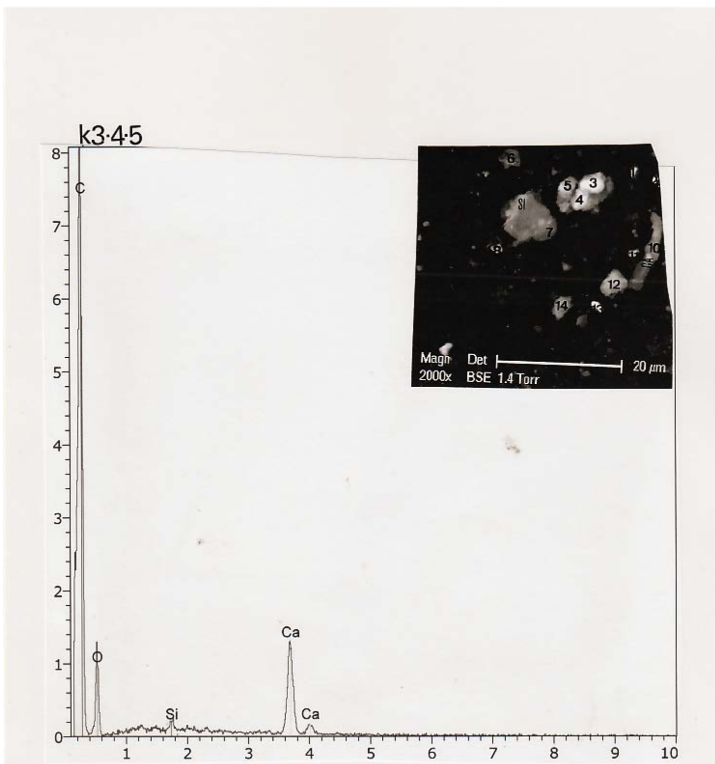

Figure 11. The k 3-4-5 Coccolith. *Above*: SEM1 photograph (2000×), in BSE, of the upper part of the K area showing k3-4-5. *Below*: The k3-4-5 spectrum.

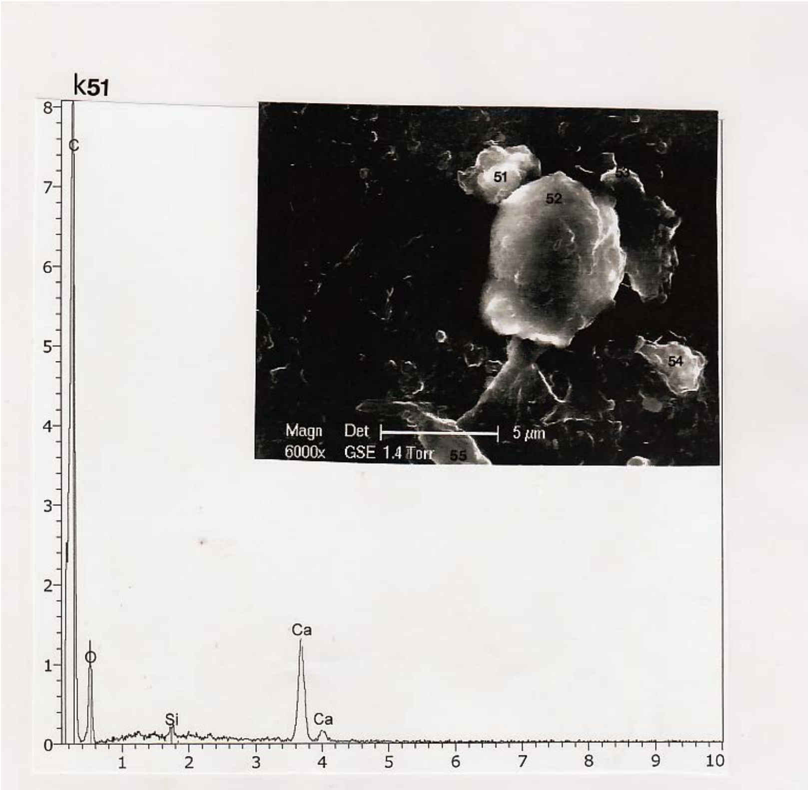

Figure 12. The k51 Coccolith. *Above*: SEM1 photograph (6000×), in GSE, of some lower part of the K area showing k51. *Below*: The k51 spectrum.

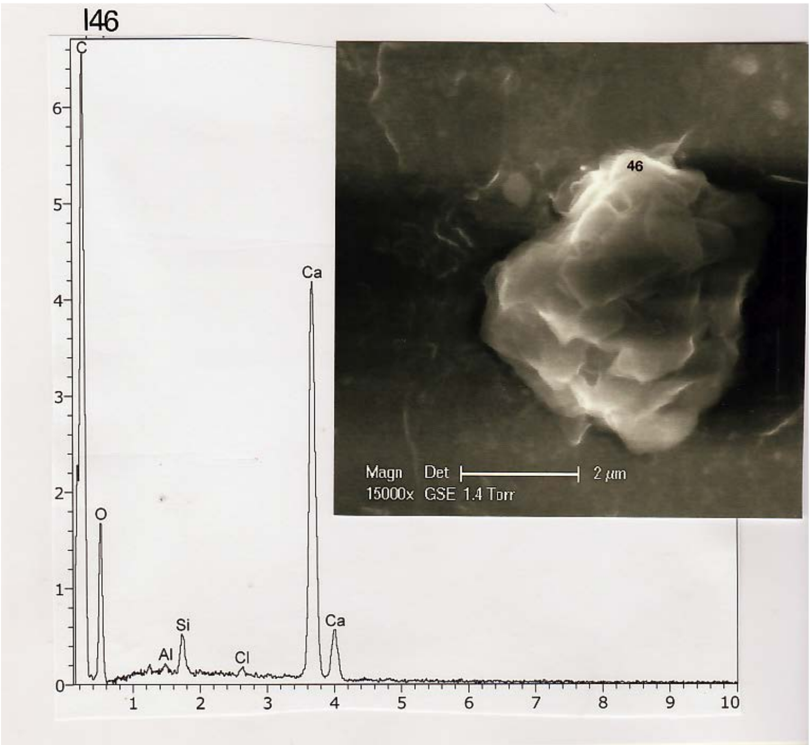

Figure 13. The l46 Coccolith. *Above*: SEM1 photograph (15,000×), in GSE, of the left L area showing l46. *Below*: The l46 spectrum.

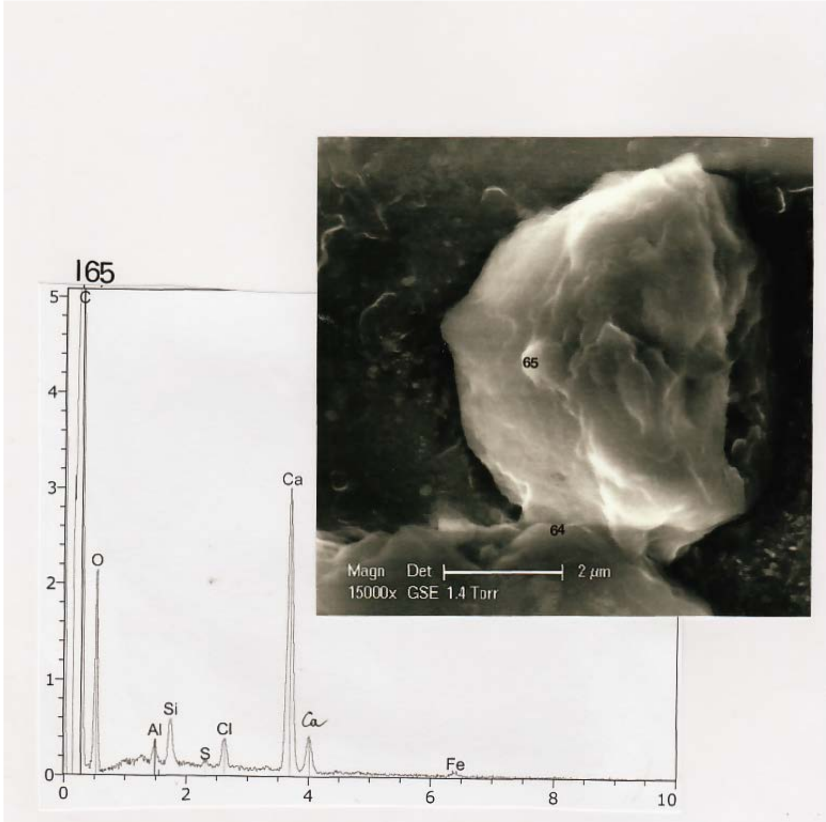

Figure 14. The l65 Coccolith. *Above*: SEM1 photograph (15,000×), in GSE, showing the l65 particle in the right part of the L area; l64 is an alumino-silicate, iron-rich. *Below*: The l65 spectrum.

Photograph of **Figure 15** shows the r25 Coccolith, located in the right middle part of the R area. It is triangular, of 4.5 µm and formed of three plaques.

There are four Coccoliths in the S area: s3, s4, s7 and s12. The Coccoliths s3, s4 and s7 are located in the upper part of the S area. The s3 Coccolith is pentalobed, of 6 µm and formed of five micro-plaques. The s3 Coccolith is trilobed, of 4.5 µm and formed of three micro-plaques. The s7 Coccolith is bilobed, of 4.5 µm and formed of two micro-plaques.

Photograph of **Figure 16** shows some of the right part of the S area with the s12 Coccolith. Neighbouring particles in that area are: s10, a silice; s11, a fine grained calcium carbonate; s13, a micro-ball of calcium chloride; s14, a lapis-lazuli; s15, a gypsum; s16, a kaolinite (Lucotte, 2023). The s12 Coccolith is pentalobed, of 12.5 µm and formed of eight plaques.

Table 2 gives the list and characterization of the thirty-two detected particles of Coccoliths.

Their spectra correspond to that of a calcium carbonate. As for the marble particles, their spectra show often little peaks or traces of silicum, aluminium, magnesium and chlorine.

When visible their colours are generally white, or pale-yellow (the q8 Coccolith is black, because it contains iron oxide).

Table 2. List and characteristics of the thirty-two particles of Coccoliths located in the areas of the triangle.

Particles	Areas	Nomenclature	Forms	Plaque numbers	Maximal lengths (in µm)	Spectra (calcium carbonate)	Colours	Peculiarities
1	A	a10	tetralobed	4	on 4	+	not visible	
2	A	a36-36’	oval	≈20	9.5		not visible	
3	B	b50	multilobed	9	on19	+	white	
4	B	b67	trilobed	5	9	+	not visible	
5	B	b74’	oval	8	6.5	+	white	on the left part of b74
6	D	d30	rounded	10	6	+	white	
7	D	d34	oval	7	9.5	+	white	eroded
8	E.a	e3	cupuliform	7	8	+	masked	
9	E.e	e114	pentalobed	6	8	+	white	
10	F	f1	cupuliform	7	7.5	+	white	
11	F	f3	oval	>20	6	+	pale-yellow	eroded
12	H	h19	elongated	7	10.5	+	white	
13	I	i5	trilobed	16	8.5	+	white	
14	I	i6	pentagonal	8	7	+	white	
15	I	i30	rounded	3	4.5	+	white	
16	I	i48	pentalobed	6	10	+	white	
17	I	i56	trilobed	12	5	+	white	
18	J	J65	oval	>20	9.5	+	white	
19	K	k3-4-5	oval	7	10.5	+	white	
20	K	k51	ovoïd	6	4.5	+	white	
21	L	l46	quadrilobed	>15	5.5	+	white	
22	L	l51-52-53	oval	8	8	+	white	
23	L	l65	form of an urn	>7	7.5	+	pale-yellow	iron traces
24	M	m13	quadrilobed	6	6.5	+	white	with barium
25	M	m40	triangular	>7	8	+	white	with barium and iron
26	M	m43	pentalobed	>12	9.5	+	pale-yellow	with barium and iron
27	Q	q8	oval	>8	2.5	+	black	with iron
28	R	r25	triangular	3	4.5	+	white	
29	S	s3	pentalobed	5	6	+	clear-yellow	
30	S	s4	trilobed	3	4.5	+	clear-yellow	
31	S	s7	bilobed	2	4.5	+	white	
32	S	s12	pentalobed	8	12.5	+	white	

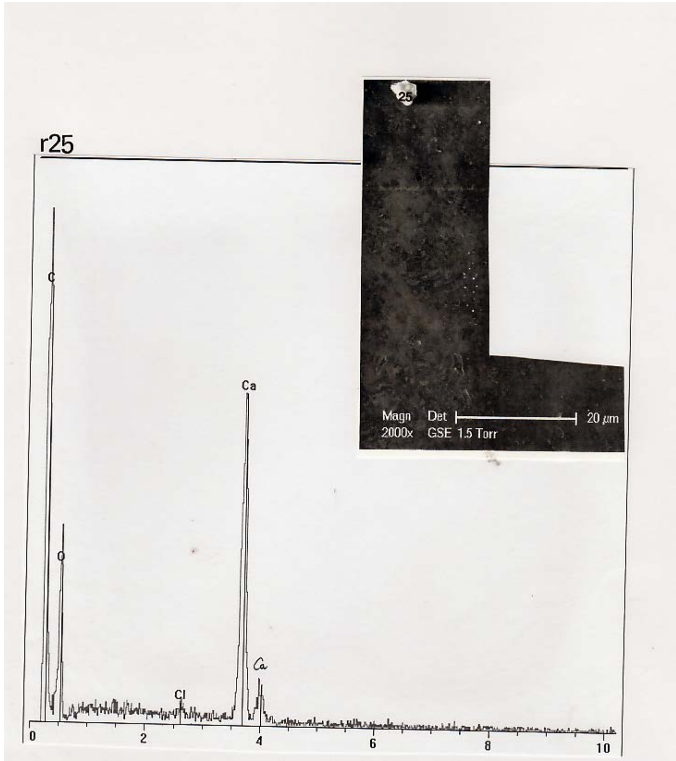

Figure 15. The r25 Coccolith. *Above*: SEM1 photograph (2000×), in GSE, of the middle part of the R area showing r25. *Below*: The r25 spectrum.

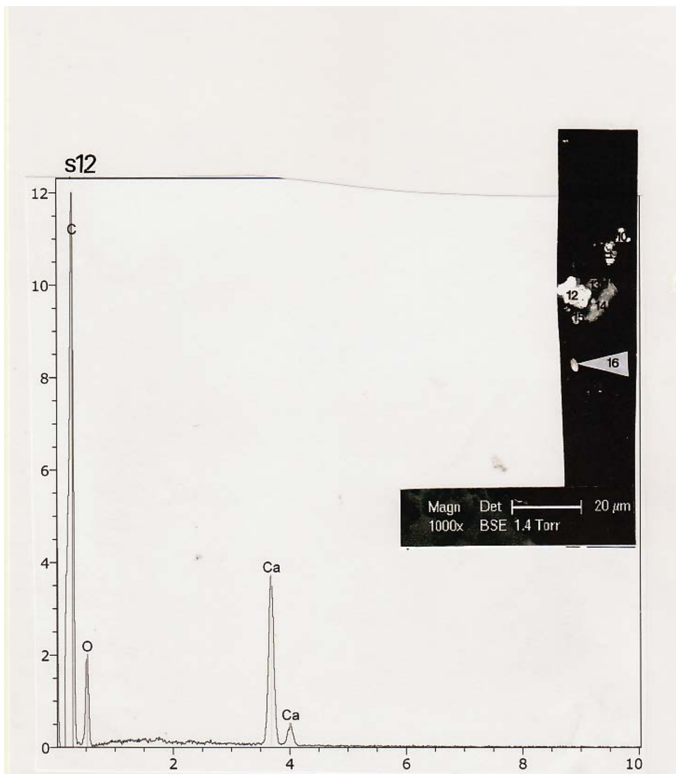

Figure 16. The s12 Coccolith. *Above*: SEM1 photograph (1000×), in BSE, of the right part of the S area showing s12. *Below*: The s12 spectrum.

3.3. White of Lead

From the Roman period onwards (it was called "cerussa" at that time) lead white has been by far the most important of the white pigments. The term of ceruse can generally be used for any lead-based white pigment and can be extended to describe lead chloride oxides, lead phosphates and lead sulphates, but it usually refers to lead carbonate by hydroxide: $2PbCO_3$. Pb $(OH)_2$. Ceruse *sensus stricto* is a lead carbonate of chemical formula (neutral form): PbCo3 (Dun, 1975).

This pigment is permanent, relatively stable (it turns yellow with time) in all medias.

The concern over lead poisoning increased during the Industrial Revolution. Although lead white continued to be marketed, its presence sharply decreased in the first half of the 20th Century (from nearly 100% to less than 10% by 1945) and was widely abandoned in the period after World War 2.

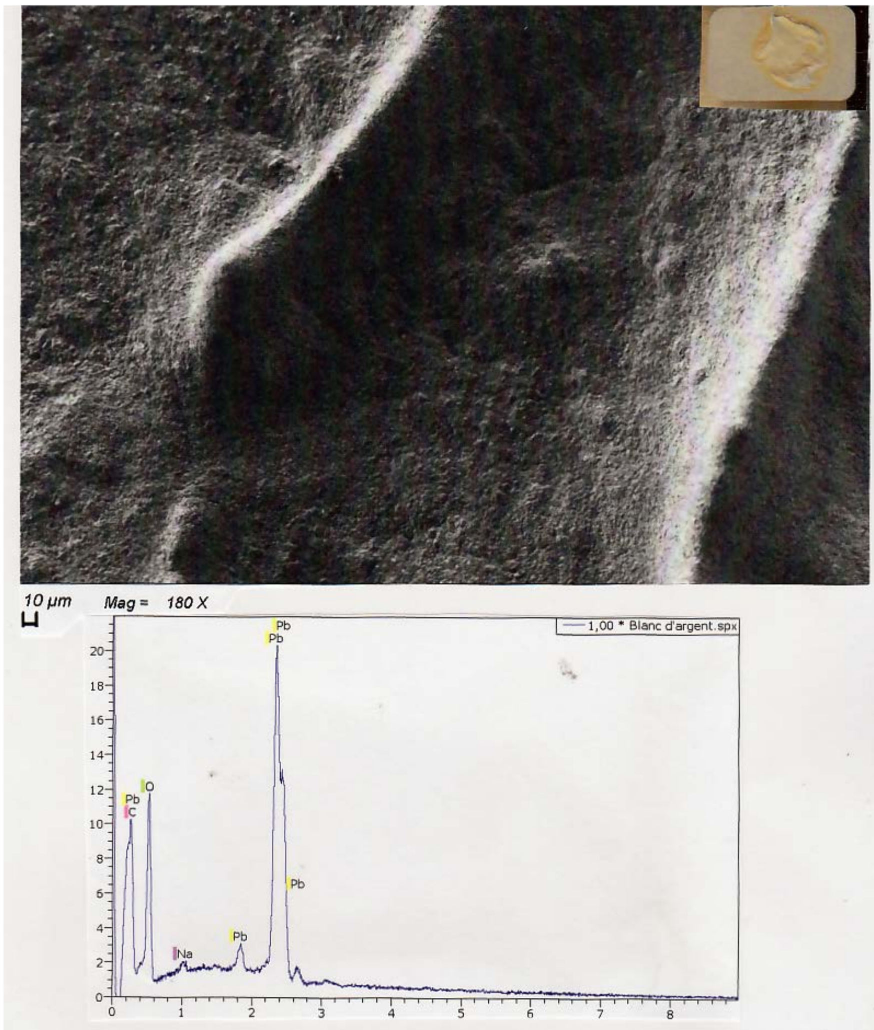

Figure 17. The varnish of ceruse of reference. *Above*: SEM3 photograph (180×) of this varnish; insert shows that it is of clear-yellow colour. *Below*: global spectrum of the varnish. C: carbon; O: oxygen; Na (traces): sodium; Pb (five peaks): lead.

Figure 17 summarizes results obtained concerning a commercial ceruse of reference. It is named "blanc d'argent", a clear-yellow varnish. The SEM3 photograph of the figure shows that it is constituted of very fine particles included in the varnish pastry. The global spectrum of this varnish is that of a ceruse.

Often in the particles of the triangle, ceruse is stabilized by pyromorphite, of general formula $Pb_5((PO_4)_3Cl$, which is not a pigment.

The first sort of ceruse particles found on the triangle surface is the formation located above b45 (a hidden Diatom) and b44 (a calcium carbonate) and below b43 (a peridot). The photograph of Figure 18 shows some right part of the B area of the triangle containing this formation. It is formed of multiple ceruse particles, of different sizes and forms. Spectra of the biggest ones (**PB1**, **PB2** and **PB3**) contain lead (Pb) as the main element, and phosphorous (P) and chlorine (Cl) as elements of the pyromorphite. All the other little particles (up to 50) located on b43, b45 and between these two are also ceruses.

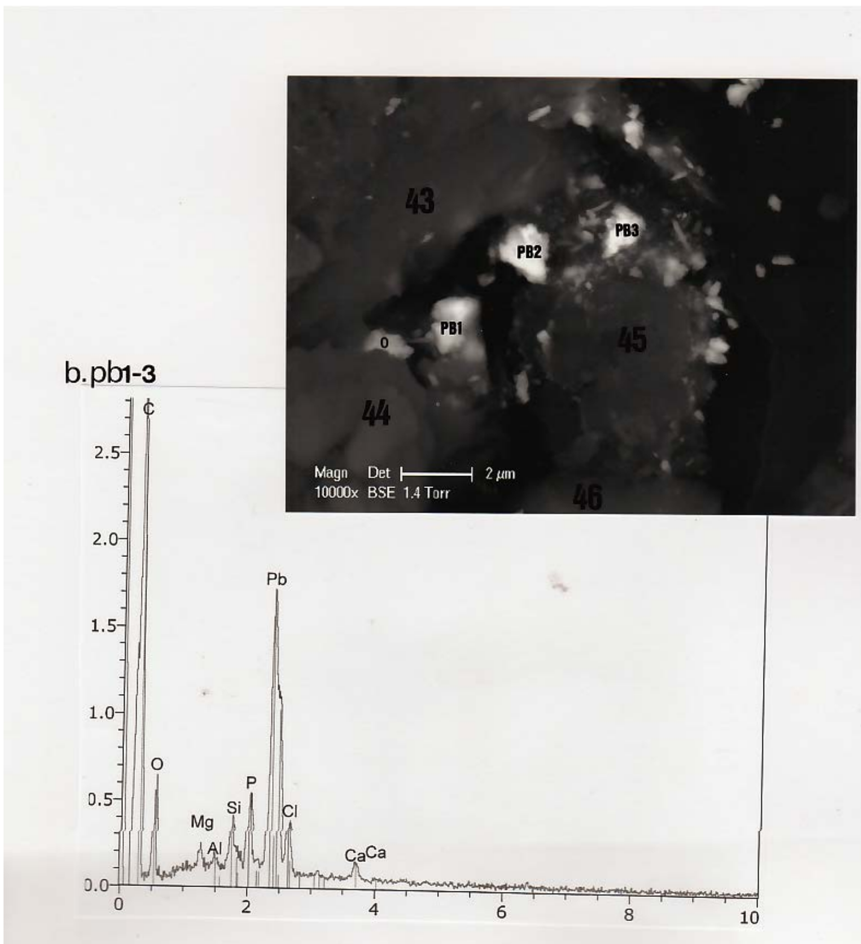

Figure 18. Particles of the first form of ceruse. *Above*: SEM1 photograph (10,000×), in BSE, of some of the right part of the B area, showing three great particles (**PB1**, **PB2**, **PB3**) and all the other little particles located on b43, b45 and between them. *Below*: HR spectrum of b-PB1-3. C: carbon; O: oxygen; Mg: magnesium; Al: aluminium; Si: silicium; P: phosphorous; Pb (the main peak): lead; Cl: chlorine; Ca (two peaks): calcium.

This formation is yellow in optic microscopy.

Other ceruses founded on the triangle surface are of a second type; they are formed of small and rounded sub-particles (micro-balls) of lead. The photograph of **Figure 19** shows some part of the M area containing particles m39 and m41. Other neighbouring particles in that area are: m17, a crystal; m31, a lapis-lazuli; m32, a double carbonate; m33, a gypsum; m35, that is organic; m42, a micro-ball of barium sulphate and of cadmium sulphure contaminated by lead; m40 and m43, two Coccoliths; m44, a Diatom; m45 and m46, two steatites; m47, a double carbonate.

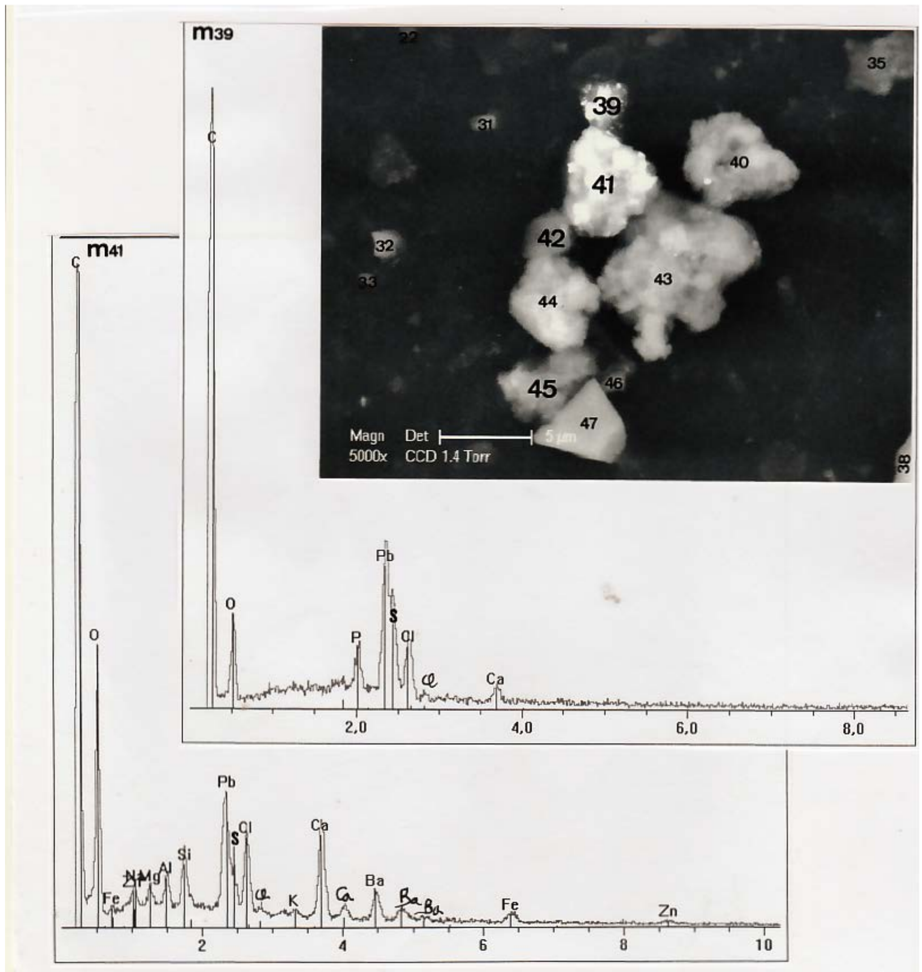

Figure 19. Particles m39 and m41 of the second form of ceruse. *Above*: SEM2 photograph (5000×), in CDD, of the lower part of the M area showing particles m39 and m41. *Upper spectrum*: spectrum of the m39 particle. *Lower spectrum*: spectrum of the m41 particle. C: carbon; Fe (two peaks): iron; Zn (two peaks): zinc; Na: sodium; Mg: magnesium; Al: aluminium; Si: silicium; P: phosphorous; Pb (main peak): lead; S: sulphur; Cl (two peaks): chlorine; K: potassium; Ca (two peaks): calcium; Ba (three peaks): barium.

This photograph, in CCD, shows that the m39 and m41 particles contain many small and rounded sub-particles (micro-balls).

The spectrum of the m39 particles contain Pb, P and Cl as main elements; it can be a pyromorphite. The spectrum of m41 contains also the same main elements, but not phosphorous; this last contains also barium sulphate and the zinc (Zn) element, in the form of zinc sulphure: a zinc white pigment named lithopone.

The m39 and m41 particles are white in optic microscopy.

Photograph of **Figure 20** shows another part of the M area containing the m30 particle, a micro-ball located between the m41-44 region and that of the m13 Coccolith and the m14 pollen. The m30 spectrum contains mainly Pb. Its colour is white in optic microscopy.

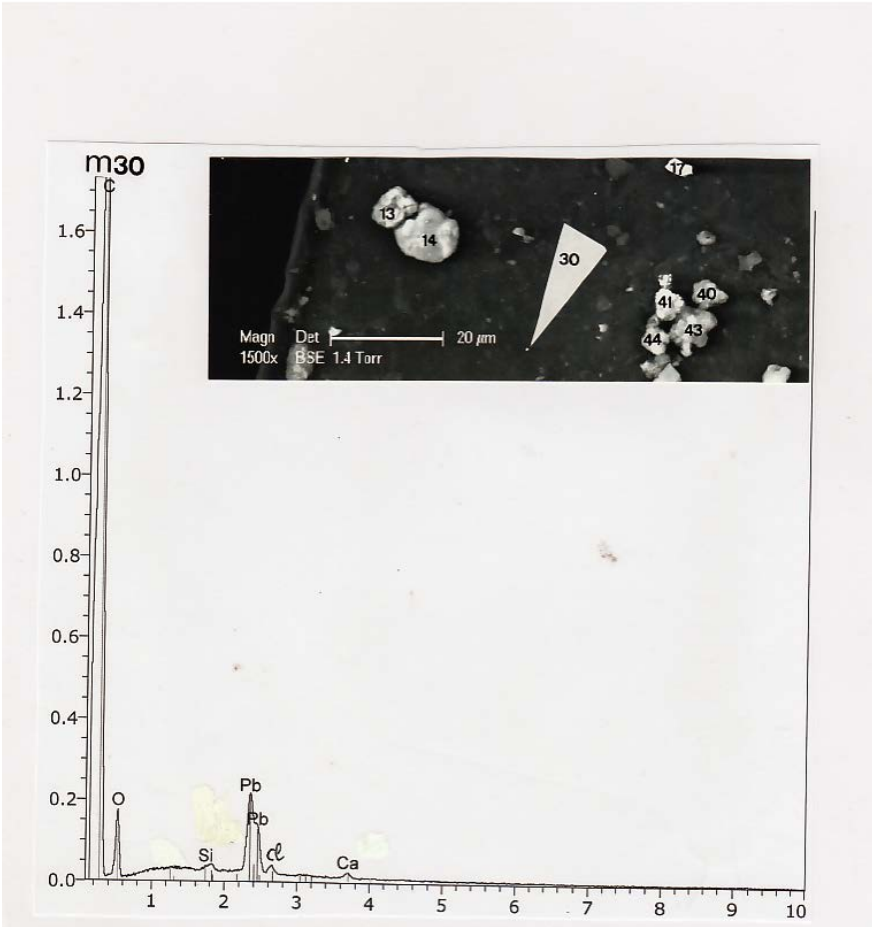

Figure 20. The m30 particle. *Above*: SEM1 photograph (1500×), in BSE, of the lower part of the M area showing the m30 particle (triangle). *Below*: HD spectrum of the m30 particle.

The strongest evidence of ceruse is that of the lead micro-balls in the paint binder e34 which contains also phosphorous of a pyromorphite. The lower photograph of **Figure 21** shows some part of the E.a area containing this binder. That particle contains up to thirteen lead micro-balls (particle e40, located near the right border of e34, is also a lead micro-ball). The spectra of the micro-balls of the group 10 contains lead as the main element.

In optic microscopy the e34 particle appears as covered by the white micro-ball points. The e49 colour is also white in optic microscopy.

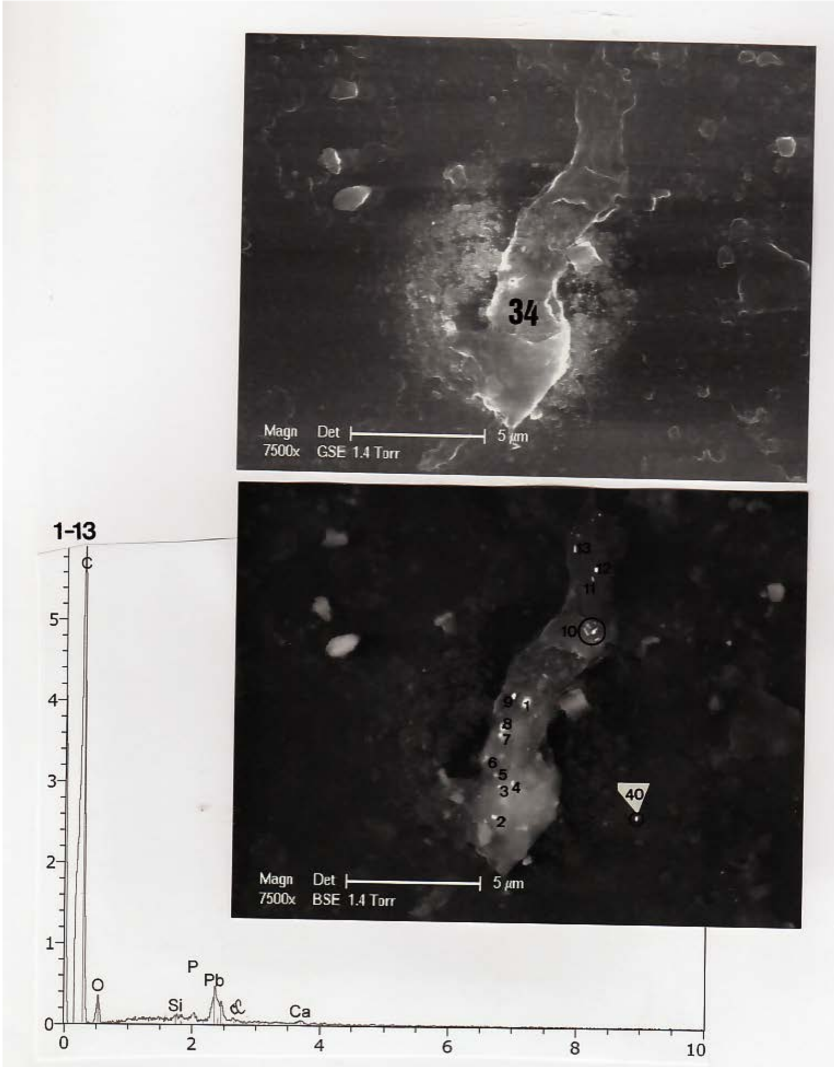

Figure 21. Ceruse micro-balls on the paint binder formation e34. *Upper photograph*: SEM1 photograph (7500×), in GSE, of the paint binder formation e34 located in the upper right part of the E.a area. *Lower photograph*: the same SEM1 photograph, but in BSE. The "white" sub-particles numbered 1-13 are located on e34; the e40 sub-particle is located outside of e34. *Below*: Spectra of e1-13 (and of e40)—only one of them is represented—sub-particles. The EDX analysis concerned initially the sub-particles group named as 10 (in the circle).

The photograph of Figure 22 shows some part of the F area containing the f10 particle. Other adjacent particles in that area are: f8, a series of piled up cylindric Diatoms; f17, a cylindric Diatom; f13-14, a calcium phosphate; f11, an illite (Lucotte, 2023). The f10 spectrum contains mainly the lead element. This particle is white in optic microscopy.

Table 3 gives the list and characterizations of the formation and of the six particles of ceruse. The formation is of type 1 and the particles of type 2. The formation is yellow in optic microscopy and the particles are of white colour.

There are some other lead micro-balls in the triangle (for example: g78, with barium and cadmium, f30 and j64) but they are not lead whites.

Figure 22. The particle f10. *Above*: SEM1 photograph (800×), in BSE, of the left part of area F, showing the f10 particle. *Below*: Spectrum of the f10 particle.

Table 3. List and characteristics of the formation and the six particles of ceruse located in the areas of the triangle.

Formation and particles	Areas	Locations and nomenclature	Compositions	Types (1 or 2)	Lengths (in µm)	Spectra	P	Cl	Colours
1	B	between b43, b44 and b45	4 great plaques (0 - 4) > 50 micro-plaques	1	on 10	+	+	+	yellow
2	M	m39	many (at least 11) are micro-balls	2	2.5	+	+	+	white
3	M	m41	many (more than 30) are micro-balls	2	2	+	-	+	white
4	M	m30	micro-ball	2	0.5	+	-	+	white
5	E.a	e34	>13 micro-balls	2	on 12.5	+	+	traces	white
6	E.a	e40	micro-ball	2	0.5	+	+	traces	white
7	F	f10	micro-ball	2	0.5	+	-	+	white

3.4. White of Zinc

In the second half of the 18th Century, an effort began to find viable substitutes for lead white. The search was oriented in particular towards investigating zinc oxide (ZnO). Zinc oxide as white pigment was first commercialised by Winsor & Newton under the name of Chinese White and marketed as an artist's pigment in a watercolour medium. Shortly thereafter it was improved for use as white pigment.

White of zinc is a very pure white, but with-little opacity. It had a further advantage over lead-based pigments because it does not get black in the presence of hydrogen sulphide.

Figure 23 summarizes results obtained concerning a commercial white of zinc of reference. It is named "blanc de zinc", a white powder. The SEM photograph of the figure shows that it is constituted of very fine particles and of other (bigger) chiboarded particles. The global spectrum of this powder is that of a white of zinc.

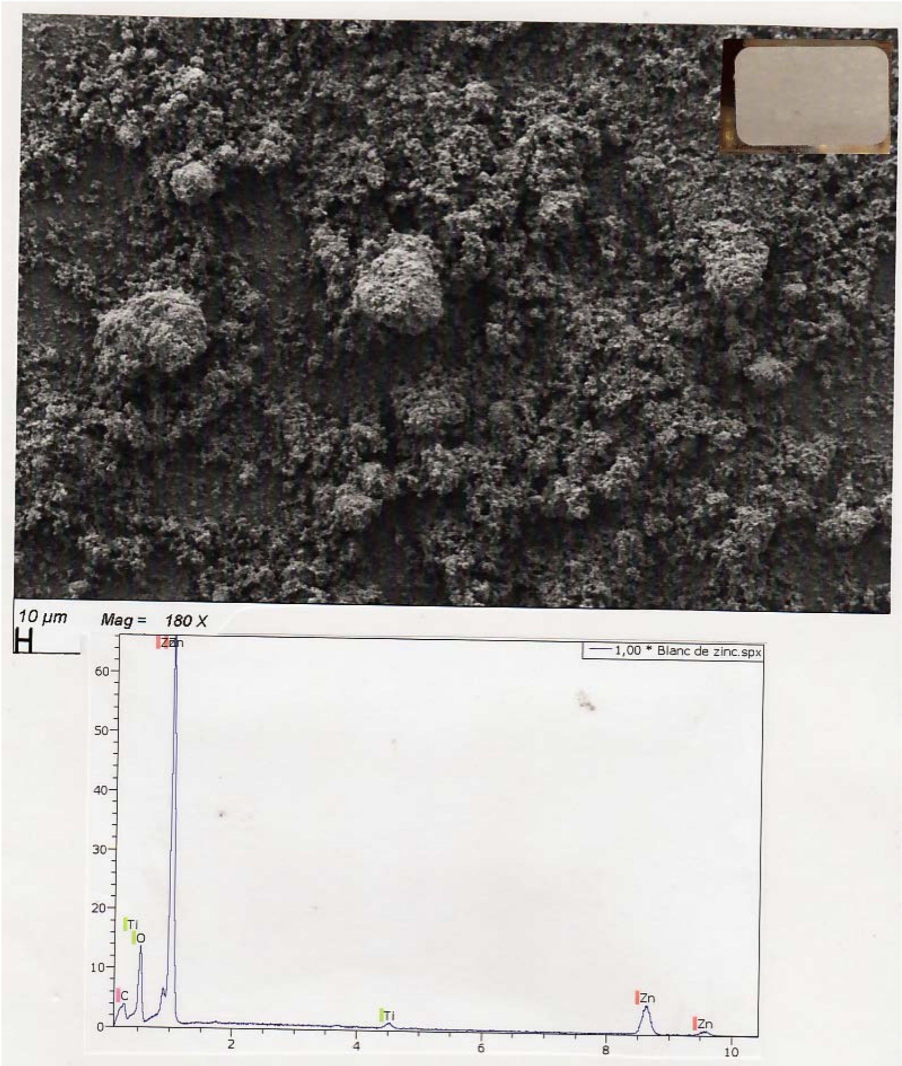

Figure 23. The "blanc de zinc" of reference. *Above*: SEM3 photograph (180×) of this powder (insert: this white powder). *Below*: Global spectrum of this powder. C: carbon; Ti (traces of contamination): titanium; Zn (four peaks): zinc.

There is only one evidence of zinc oxide particle on the triangle surface: that of the j8 particle. The photograph of **Figure 24** shows some of the upper part of the

J area with j8. Other adjacent particles in that area are: j1, a spore; j2, which is organic; j3, a calcite; j4, a calcium carbonate; j5, a barium sulphate; j6 and j7, two gypsums; j9, a silice; j10, an Ostracod; j11, a marble; j12 and j13, two gypsums.

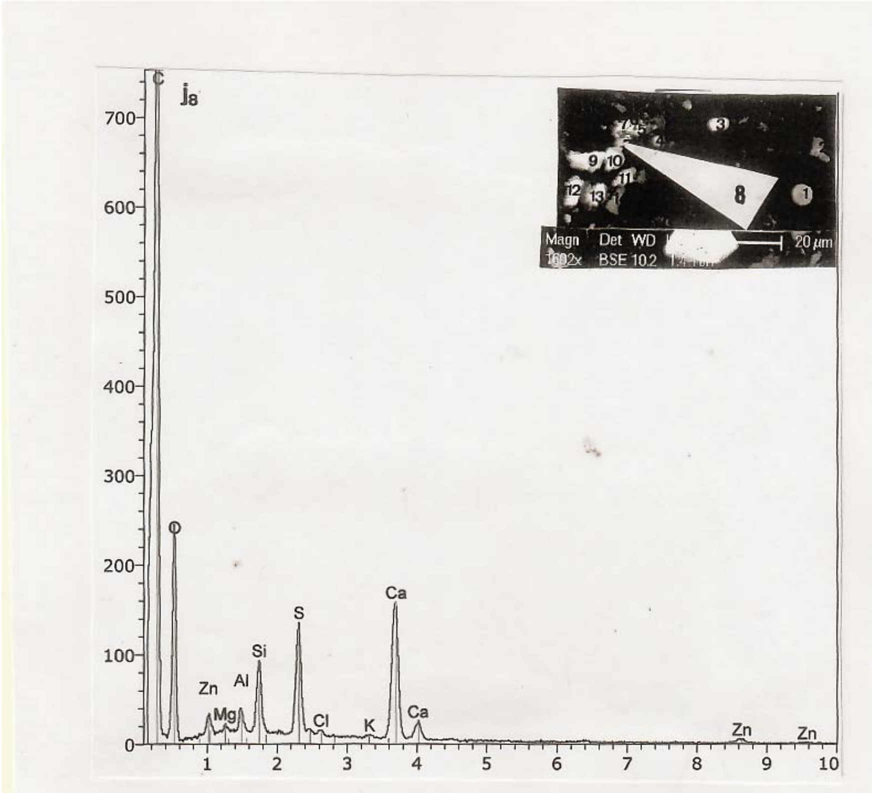

Figure 24. The zinc oxide particle j8. *Above*: SEM1 photograph (1602×), in BSE, of some part of the J area showing j8. *Below*: The j8 spectrum. C: carbon; O: oxygen; Zn (three peaks): zinc; Mg (traces) magnesium; Al: aluminium; Si: silicium; Cl (traces): chlorine; K (traces): potassium; Ca (two peaks): calcium; Ba (traces): barium.

The j8 particle is small and elongated (about 3.5 µm of approximate length), fitted between j5, j6, j7 and j10. Its spectrum shows the three peaks of the Zn element and a relatively elevated peak concerning oxygen. Elevated values of the sulphur and of the main calcium peaks in the spectrum indicate gypsum (a calcium sulphate) contamination by the neighbouring j6 and j7 particles.

The j8 particle is white in optic microscopy.

Lithopone, a French white of zinc, is an equimolar mixture of zinc sulphure and barium sulphate ($BaSO_4 \cdot ZnS$). It was used in painting mainly around 1920. It had a great opacity and is excellent white pigment for watercolours, gouaches and fat pastels.

Figure 25 summarizes results obtained concerning a commercial lithopone of reference. It is a white powder. The SEM photograph of the figure shows that it is constituted of fine chipboarded particles. The global spectrum of this powder is that of a mixture of barium sulphate and zinc sulphure. As already seen, the m41 particle of the triangle contains its.

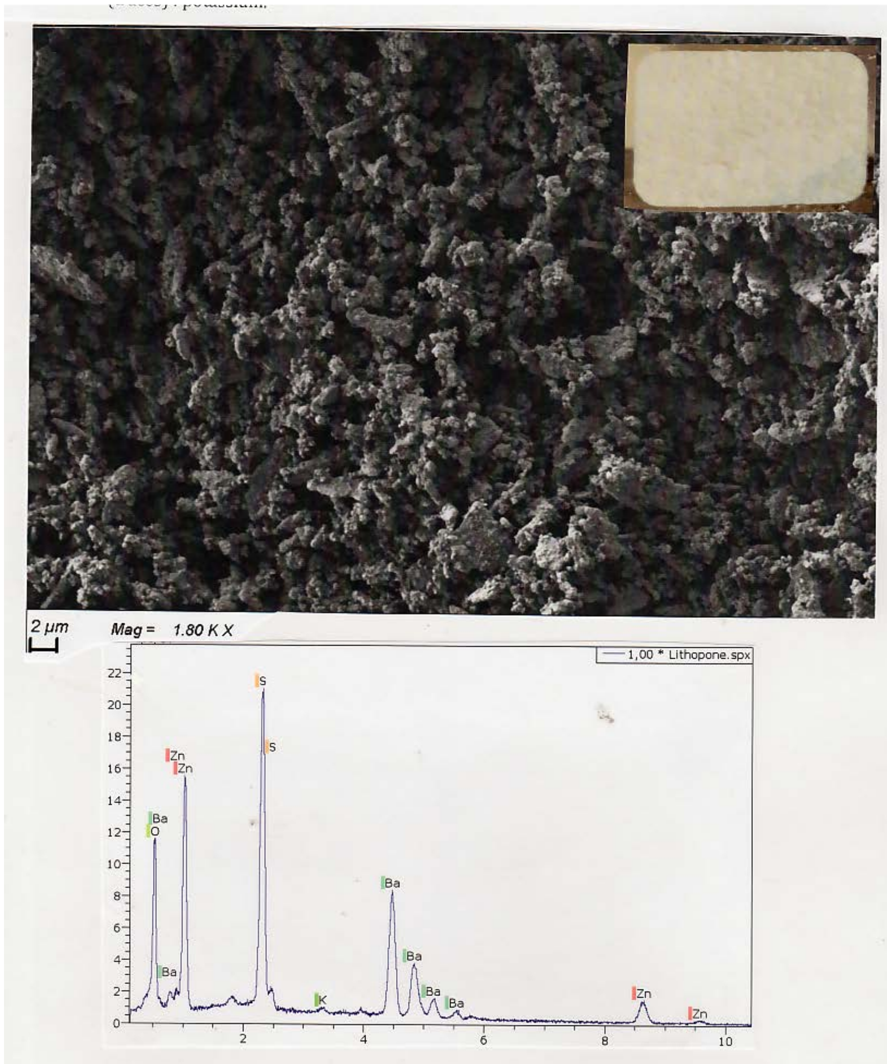

Figure 25. The lithopone powder of reference. *Above*: SEM3 photograph (1800×) of the powder (insert: this powder is white). *Below*: Global spectrum of the powder. O: oxygen; Ba (six peaks): barium; Zn (four peaks): zinc; S (two peaks): sulphur; K (traces): potassium.

The zinc sulphate is a white crystalline product, of chemical formula $ZnSO_4$. It is sometimes used in painting (actually mainly for white washing of the paper).

Figure 26 summarizes results obtained concerning a commercial zinc sulphate. It is a white powder, named as "sulphate de zinc". The SEM photograph of the figure shows that it is constituted of big (of about 1 mm of dimensions) particles of a white powder. The global spectrum of this powder is that of a zinc sulphate.

There is only one evidence of zinc sulphate particle on the triangle surface: that of the particle r(gy-11). The photograph of Figure 27 shows, in some of the upper part of the R area, the r(gy-11) particle. Other neighbouring particles in that area are: gy-8, a calcium carbonate; gy-9, a micro-ball of iron oxide; gy-10-12-13-14-15-16-17, 18 and 19 are gypsums; gy-20 is an Ostracod.

The r(gy-11) particle, small (2.5 µm) and elongated, is located between the gypsums gy-10 gy-12 and gy-13. The r(gy-11) spectrum shows the three peaks of the zinc element, an important peak of the oxygen element and a less important peak of the sulphur element.

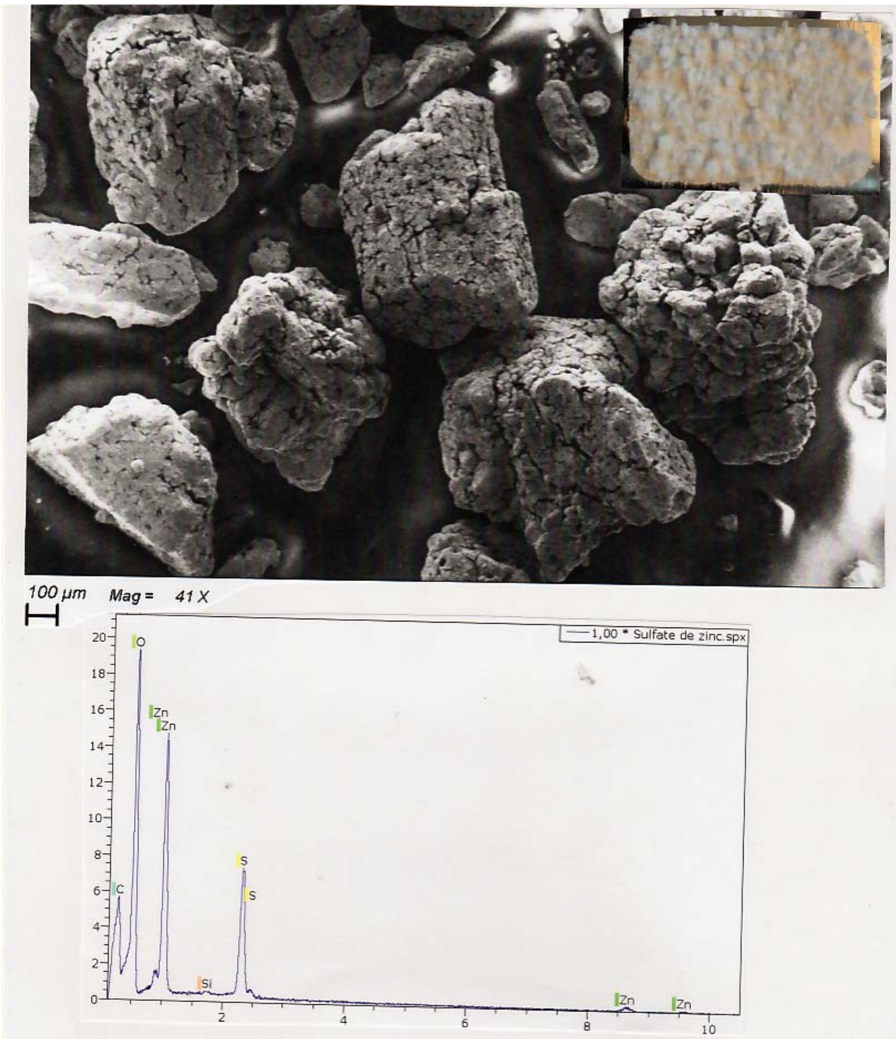

Figure 26. The "sulphate de zinc" powder of reference. *Above*: SEM3 photograph (41×) of this powder (insert: a white powder of voluminous particles). *Below*: Global spectrum of the powder. C: carbon; O: oxygen; Zn (four peaks): zinc; Si (traces): silicium; S (two peaks): sulphur.

The r(gy-11) particle is white in optic microscopy.

3.5. White of Titanium

White of titanium is titanium dioxide, of the chemical formula TiO_2. It is the white pigment that is the most commonly used actually in painting (since 1916). TiO_2 pigment is chemically inert, resists to fading in sunlight and is very opaque. Alumine (Al_2O_3) and silica (SiO_2) are the main post treatments used as medias for titanium painting.

Figure 28 summarizes results obtained concerning a commercial white of titanium reference. It is named "blanc de titane", a white powder. The SEM photograph of the figure shows that it is constituted of rounded particles of about 200 nm of diameter. The global spectrum of this powder is that of titanium dioxide.

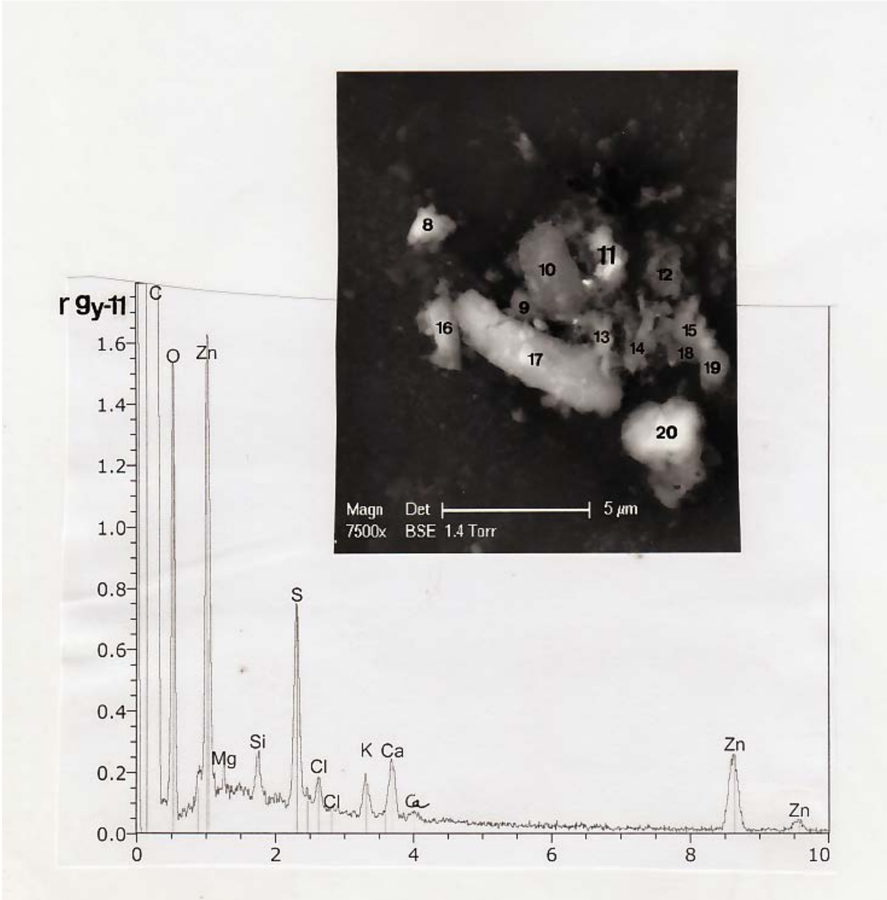

Figure 27. The r(gy-11) particle. *Above*: SEM1 photograph (7500×), in BSE, of some of the upper part of the R area showing r (gy-11). C: carbon; O: oxygen; Zn (three peaks): zinc; Mg: magnesium; Si: silicium; S: sulphur; Cl (two peaks): chlorine; K: potassium; Ca (two peaks): calcium.

It is important to make the distinctions between titanium used in painting, mineral titanium and "industrial" titanium. Mineral titanium is a common element of some clays (Lucotte, 2023), where it accompanies iron; mineral titanium occurs also in some phosphorites (Lucotte et al., 2024) and even in some lapis lazuli particles. "Industrial titanium" occurs in some objects of compact form (a good example of this sort of "industrial titanium" on the triangle surface is the microfilament a15 in the A area).

A typical example of titanium dioxide pigment found on the triangle surface is the h13 formation (**Figure 29**); the photograph of this figure shows that it has the appearance of a paint film, large at one extremity and narrow at the other. Its spectrum has the three peaks of the titanium element, and the two peaks of aluminium and silicium. It is located on an Ostracod for its greater extremity, and on a Diatom for the other (that explaining the elevated values of the calcium and the silicium elements in its spectrum); the location of a calcium carbonate at its medium right part explains also its elevated value in the calcium element.

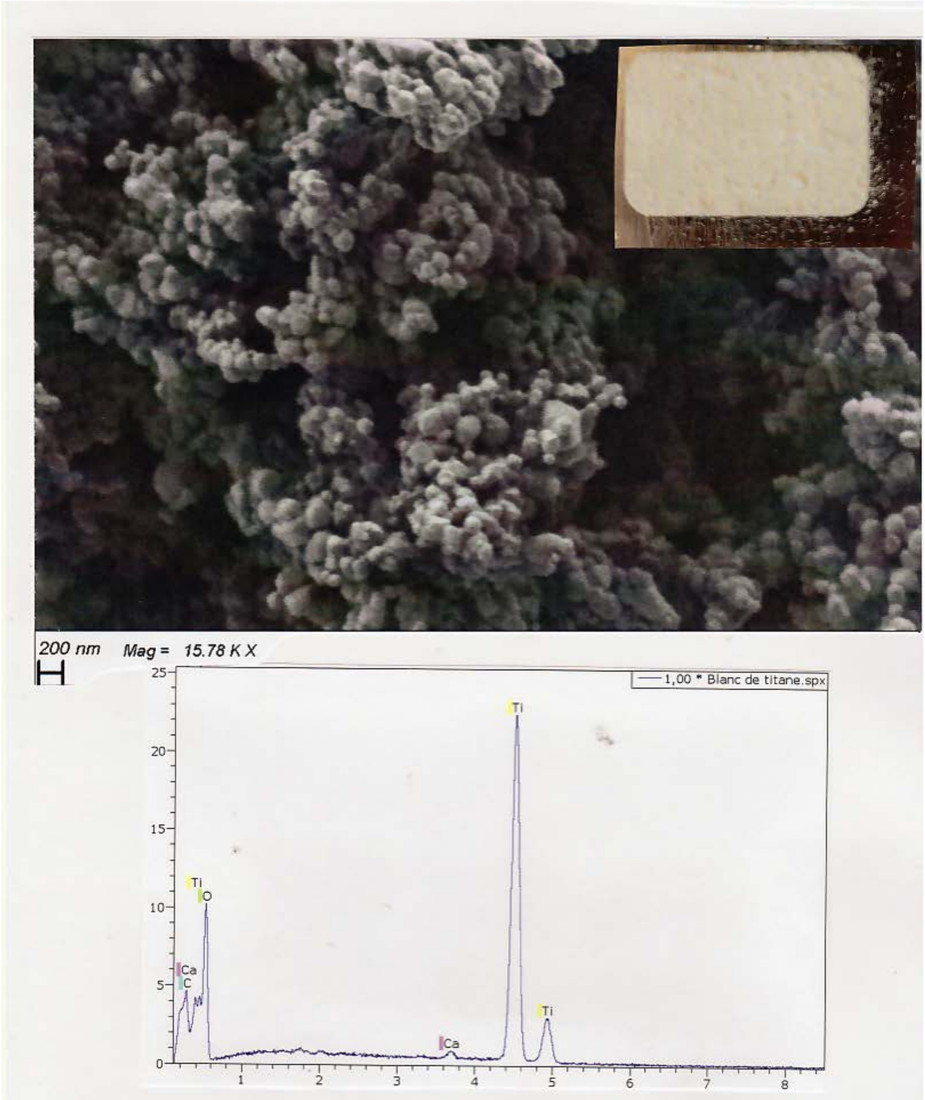

Figure 28. The white of titanium powder of reference. *Above*: SEM3 photograph (15,780×) of the powder (insert: this powder is white). *Below*: The global spectrum of the powder. C: carbon; Ti (three peaks): titanium; O: oxygen; Ca: calcium.

This photograph illustrates also presences of mineral and "industrial titanium" in neighbouring particles of h13: mineral titanium traces in h16, which is a clay; "industrial titanium" in h15, which is a sodic glass; the h14'particle is an altered calcic glass fragment containing titanium and iron.

Photograph of **Figure 30** shows some part of the A area, with particles a18 (a clay), a 19 (an Ostracod) and a20 (a steatite); a 21 is a spore. There is a titanium micro-scale (**T**) on the left border of a18. Its spectrum contains the three titanium peaks and one iron peak. The colour of the **T** micro-scale is pink (because of iron-oxide) in optic microscopy.

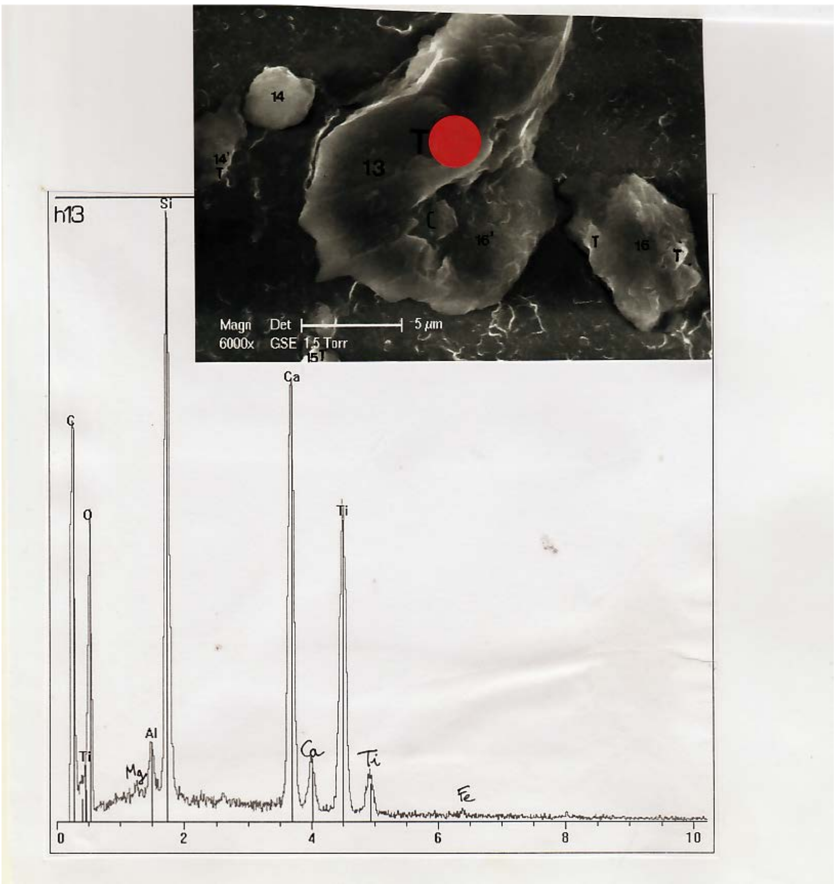

Figure 29. The h13 titanium paint film. *Above*: SEM1 photograph (6000×), in GSE, of some of the higher part of the H area showing h13 (Ti: titanium; Si: silica; C: calcium carbonate); the red point on h13 indicates the approximate location where is realized the SEM-EDX analysis. *Below*: Spectrum of h13. C: carbon; Ti (three peaks): titanium; O: oxygen; Mg: magnesium; Al: aluminium; Si: silicium; Ca (two peaks): calcium; Fe: iron (the h14 particle is a rounded calcium carbonate).

Photograph of **Figure 31** shows another part of the A area, containing the a39 particle (of barium sulphate); under a39 is the **t** micro-scale, which spectrum has the three titanium peaks; its colour is white in optic microscopy.

Photograph of **Figure 32** shows a third part of the A area, with the tripartite a40 (a feuil) a painting residue; on its surface is the micro-scale **3**, which spectrum having the three titanium peaks (and three peaks of iron); its colour is pink in optic microscopy (because of iron oxide).

Photograph of **Figure 33** shows some part of the B area, with the basis of b1, an hair (Lucotte & Thomasset, 2017). Exterior to b1 and at its right border is the micro-scale T, which spectrum had the three titanium peaks; its colour is white in optic microscopy.

Photograph of **Figure 34** shows some part of the H area containing the h28 particle (a covered Diatom). On the surface of its right inferior border is the micro-scale **T**, which spectrum had the three titanium peaks (and three iron peaks). Its colour is red in optic microscopic (because of iron oxide).

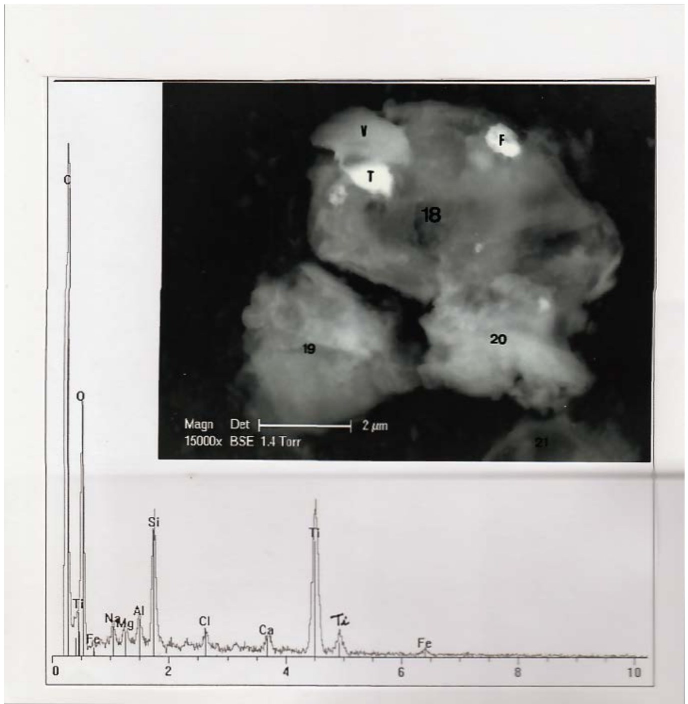

Figure 30. One micro-scale of titanium (T), loaded on the a18 particle. *Above*: SEM1 photograph (15,000×), in BSE, of the left lower part of the A area showing the titanium scale on a18 (F: iron sub-particle; V: micro-splinter of glass). *Below*: The T spectrum. C: carbon; Ti (three peaks): titanium; Fe (two peaks): iron; Na: sodium; Mg: magnesium; Al: aluminium; Cl: chlorine; Ca: calcium.

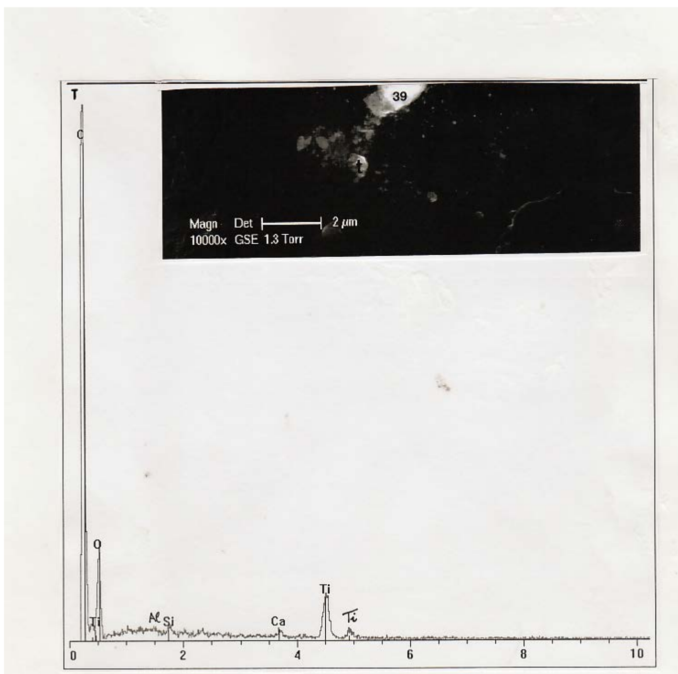

Figure 31. Micro-scale of titanium (t), located below the a39 particle. *Above*: SEM1 photograph (10,000×), in GSE, of some lower part of the A area showing this micro-scale. *Below*: Spectrum of t. C: carbon; Ti (three peaks): titanium; O: oxygen; Al (traces): aluminium; Si (traces): silicium; Ca (traces): calcium.

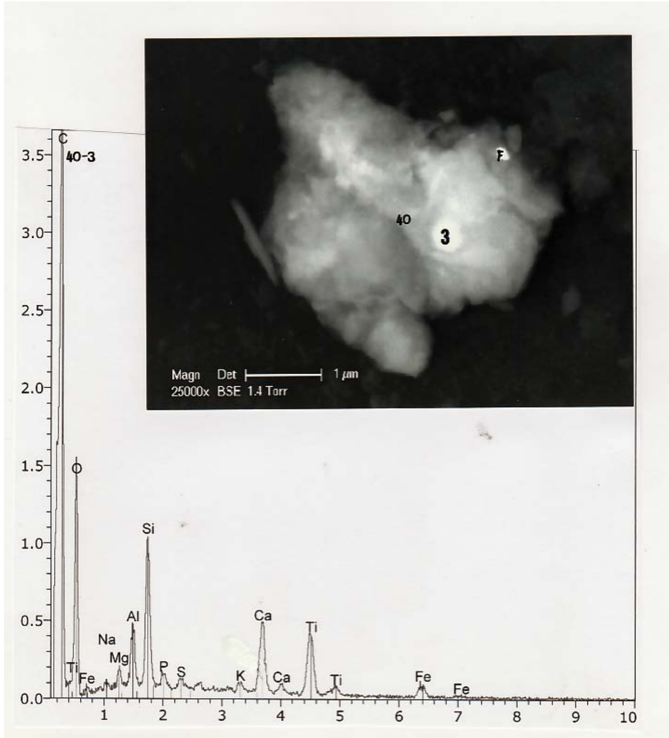

Figure 32. The a40-3 micro-scale of titanium, loaded on the a40 particle. *Above*: SEM1 photograph (25,000×), in BSE, of some lower part of area A showing the a40-3 micro-scale (F: an iron micro-plaque). *Below*: Spectrum of the a40-3 micro-scale. C: carbon; Ti (three peaks): titanium; O: oxygen; Fe (three peaks): iron; Na: sodium; Mg: magnesium; Al: aluminium; Si: silicium; P: phosphorous; S: sulphur; K: potassium; Ca (two peaks): calcium.

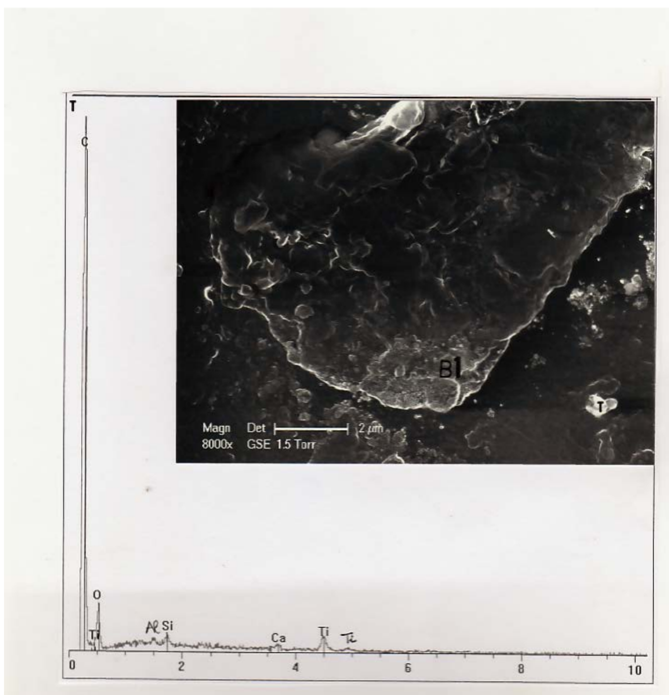

Figure 33. Micro-scale of titanium (T), near the basis of hair b1. Above: SEM1 photograph (8000×), in GSE, of the upper part of the B area showing T. *Below*: Spectrum of T.

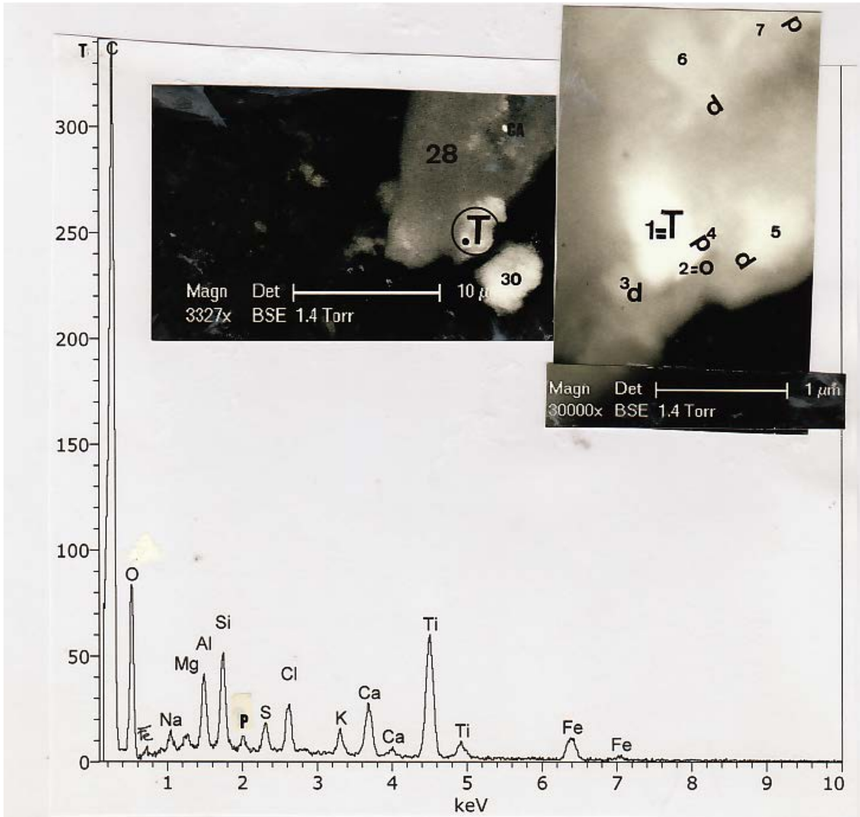

Figure 34. The titanium micro-plaque (T) located on the lower part of h28. *Left photograph*: SEM1 photograph (3327×), in BSE, of some part of the H area showing the T micro-plaque on the lower part of the h28 particle. (Ca is a calcium carbonate). *Right photograph*: SEM1 photograph (30,000×), in BSE, of the T micro-plaque; T = 1 is the micro-plaque; 2 is a gold particle (Lucotte, 2022); 3 - 7 are salts. *Below*: the HR spectrum of T.C: carbon; O: oxygen; Fe (three peaks): iron; Na: sodium; Mg: magnesium; Al: aluminium; Si: silicium; P: phosphorous; S: sulphur; Cl: chlorine; K: potassium; Ca (two peaks): calcium; Ti (two peaks): titanium.

Photograph of **Figure 35** shows some part of the J area, with particle j44 (an Ostracod). Other neighbouring particles in that area are: j42, a phosphorite with iron; j43 and j46, which are gypsums; j45, a calcite; j47, a Dynophycae; j51, an iron particle; j52 and j53, which are clays; j54, a glass; j55, a dense calcium carbonate, j56, a biotite (Lucotte et al., 2016), j62 and j64, which are calcium carbonates; j65, a Coccolith.

Spectrum of j44 had the three titanium peaks; its colour is white in optic microscopy.

Photograph of **Figure 36** shows some part of the K area, with the k44 micro-scale. Other particles in the K area are; k28, a phosphorite; k38, a blue glass; k39, an aragonite; k40, a calcite; k41, a brass formation (Lucotte & Thomasset, 2024); k42, a chlorite; k43, a phosphorite with iron, k45 and k47, that are calcium carbonates; k46, an illite (Lucotte, 2023); k48, a calcite; k49 is organic.

Spectrum of the k44 micro-particle had two titanium peaks and iron traces; its colour is white in optic microscopy.

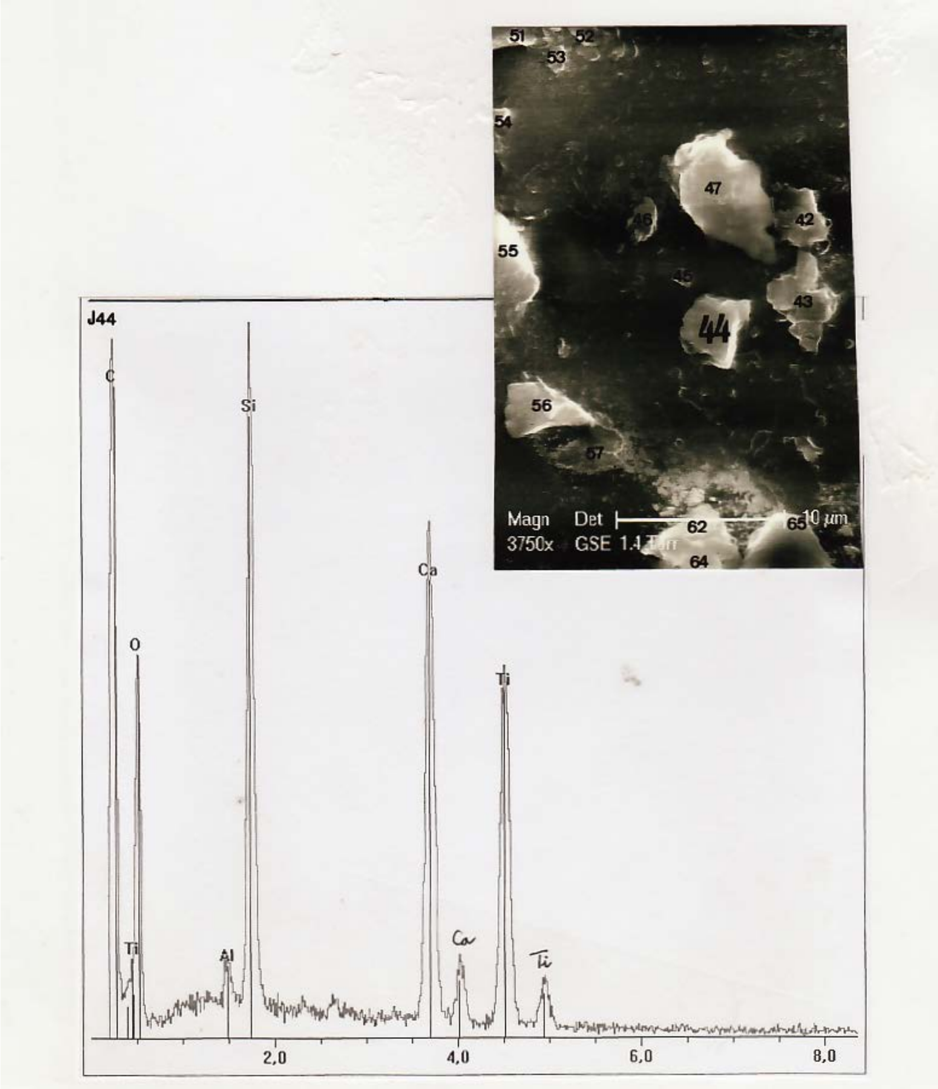

Figure 35. Titanium on j44. *Above*: SEM1 photograph (3750×), in GSE, of some of the left part of the J area showing j44. *Below*: The j44 spectrum.

Photograph of **Figure 37** shows some part of the L area containing the **T** microplaque. Other particles in vicinity are: l38, a wax; l39, an hematite (Lucotte et al., 2016); l40, a lapis lazuli; l41, a quartz. Spectrum of the **T** micro-plaque had two titanium peaks; its colour is white in optic microscopy.

Photograph of **Figure 38** shows some part of the M area, having the m53 particle (an Ostracod). Neighbouring particles in that area are: m50, a PVC plastic; m51 and m52, which are barium sulphates. The m53 spectrum had two titanium peaks, and its colour is white in optic microscopy.

Table 4 gives the list and characterizations of the ten detected particles of titanium dioxide. Their spectra are typical (TiO_2). It shows presence of the aluminium and silicium elements of the medias. Three of them (**T** on a18, **3** on a40 and **T** on h28) have iron in relatively great quantities. Their colours are generally white, but the previous three because of iron oxide.

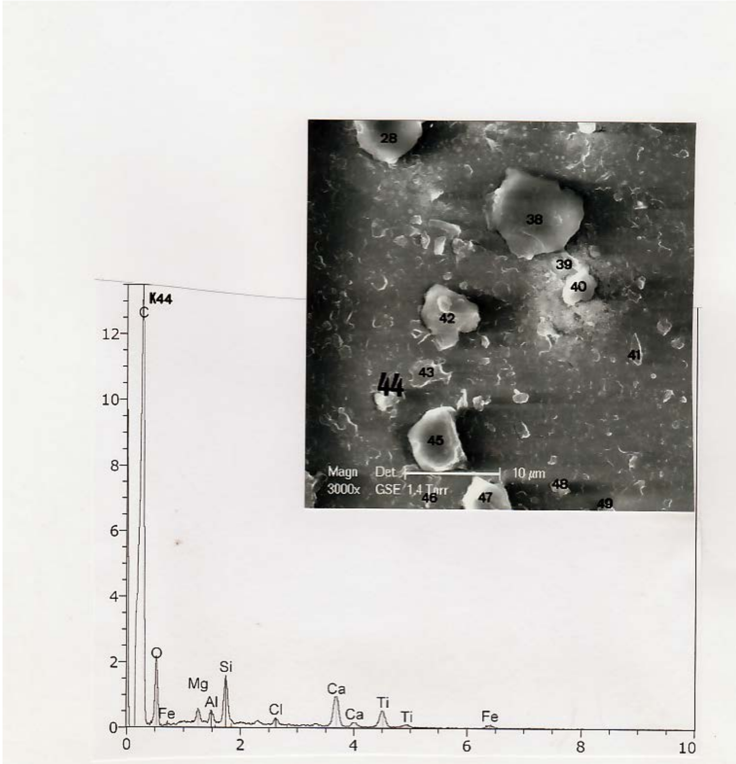

Figure 36. The micro-ball of titanium k44. *Above*: SEM1 photograph (3000×), in GSE, of a lower part of the K area showing k44. *Below*: The k44 spectrum.

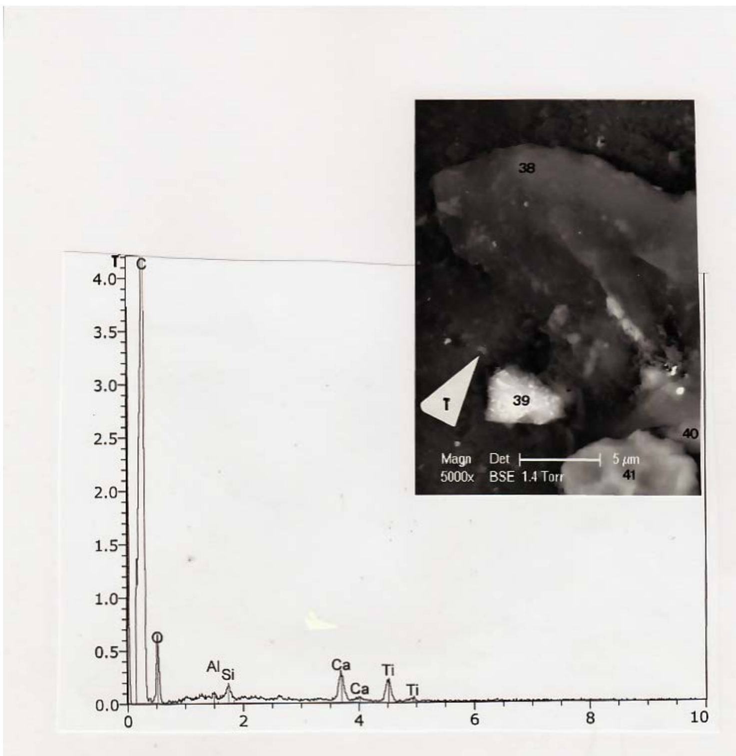

Figure 37. The titanium (T) micro-plaque, located above l39. *Above*: SEM1 photograph (5000×), in BSE, of some higher part of the L area showing T. *Below*: The T spectrum.

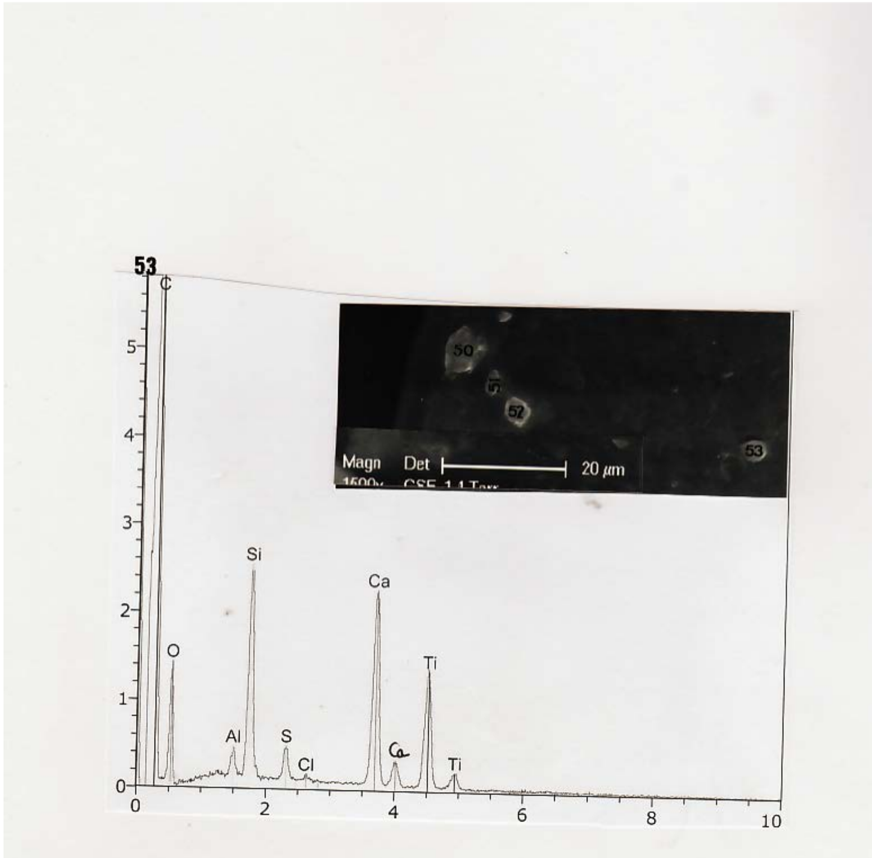

Figure 38. The m53 titanium micro-ball. *Above*: SEM1 photograph (1600×), in GSE, of some of the lower part of the M area showing m53. *Below*: The m53 spectrum.

Table 4. List and characteristics of the thirteen particles of titanium dioxide located in the areas of the triangle.

Particles	Areas	Locations	Designations	Formations	Dimensions (in µm)	Elements			Colours
						Al	Si	Fe	
1	A	on a18	T	micro-scale	1.5	+	+	+	pink
2	A	below a39	t	micro-scale	0.5	+	+		white
3	A	on a40	3	micro-scale	0.5	+	+	+	pink
4	B	at the right of the b1 basis	T	micro-scale	1	+	+		white
5	H	on three particles	h13	feuil	6 × 25	+	+	traces	white
6	H	on the h28 basis	T	micro-plaque	2 × 1.5	+	+	+	pink
7	J	on the j44 Ostracod		micro-plaque	4 × 4	+	+		white
8	K	k44		micro-ball	8	+	+	traces	white
9	L	above l39	T	micro-plaque	0.5	+	+		white
10	M	on the m53 Ostracod		micro-ball	4	+	+		white

4. Discussion

We found many particles of white pigments on the triangle surface.

A number of twenty-one micro-fragments of marble were detected. These particles are calcium carbonates, but with an elevated content of the calcium element. Such marble particles are used as white funds in ceramics and painting since the Antiquity.

A number of thirty-two Coccoliths were detected (these marine micro-organisms are characteristic of the chalk). They indicate probably some process of bleaching the TS linen (Martin & Pellerin, 2008) by chalk. Being the diversity of Coccoliths species detected, several sorts of chalk were used in the process during time.

Ceruse was the most ancient white metallic pigment used. Ceruse particles detected on the triangle are of two different forms: type 1, represented by four great plaques and more than fifty micro-plaques, are of yellow colour. Type 2, represented by micro-balls, are of white colour. Peculiarly representative is e34 (but with pyromorphite0, where about twenty ceruse micro-balls are included in a paint binder formation.

The white of zinc pigment is poorly represented on the triangle: only one particle (j8) was detected. Lithopone is possibly present in the ceruse particle m41; we have also detected one particle (r-gy-11) of zinc sulphate.

Titanium dioxide is used as a metallic white in paintings since 1916. The most demonstrating evidence of titane dioxide used as a white pigment on the triangle is the h13 paint film. Nine other micro-plaques, micro-scales and micro-balls of titanium dioxide were also detected, loaded on various particles located on the triangle surface; their colours are white, or pink, depending to their iron contents. It is a probability that the triangle was subsequently contaminated by titanium dioxide.

So, a total number of more than 185 particles of white pigments were found on the triangle surface; they contribute significantly to the laundering of this material (Coccoliths are most probably involved in a bleaching process).

5. Conclusion

We detected one hundred eighty five and fifty particles of potential white pigments on the TS surface of the triangle sample studied. These particles are micro-fragments of marble and Coccoliths (mineral pigments), ceruses, zinc oxides and titanium dioxides (metallic pigments). Almost all are white in optic microscopy. These particles, deposited on the TS at different periods of time, contribute to the white general appearance of the Turin Shroud; they correspond to secular dust depositions.

Conflicts of Interest

The authors declare no conflicts of interest regarding to the publication of this paper.

References

Dun, E. J. (1975). Lead Pigments. In R. R. Myers, & J. S. Long (Eds.), *Treatise on Coating*

Pigments (Part 1, Vol. 3, pp. 333-427). Marcel Dekker.

Heimdal, B. R. (1993). Modern Coccolithophorids. In C. R. Thomas (Ed.), *Identifying Marine Phytoplankton* (pp. 731-831). Elsevier. https://doi.org/10.1016/b978-012693018-4/50008-2

Lucotte, G. (2015). Exploration of the Face of the Turin Shroud. Pollens Studied by SEM Analysis. *Archaeological Discovery, 3,* 158-178. https://doi.org/10.4236/ad.2015.34014

Lucotte, G. (2017). The Triangle Project. *Newsletter of the British Society for the Turin Shroud, 85,* 5-14.

Lucotte, G. (2022). Gold and Silver Particles on the Turin Shroud, Studied by Scanning Electron Microscopy and Elemental Analysis. *Archaeological Discovery, 10,* 262-281. https://doi.org/10.4236/ad.2022.104009

Lucotte, G. (2023). SEM-EDX Characterization of the Little Clays Particles Deposited on the Turin Shroud Surface. *Journal of Multidisciplinary Engineering Science and Technology, 10,* 15842-15847.

Lucotte, G. (2024). Optical Microscopy and SEM-EDX Characterization of Some Little Micro-Organisms Having Chemical Formulas Similar to Those of Clays, Deposited on the Turin Shroud. *Journal of Multidisciplinary Engineering Science and Technology, 11,* 16838-16847.

Lucotte, G., & Thomasset, T. (2017). Scanning Electron Microscopic Characterization and Elemental Analysis of One Hair Located on the Face of the Turin Shroud. *Archaeological Discovery, 5,* 1-21. https://doi.org/10.4236/ad.2017.51001

Lucotte, G., & Thomasset, T. (2023). Lapis Lazuli Particles on the Turin Shroud: Microscopic Optical Studies and SEM-EDX Analyses. *Archaeological Discovery, 11,* 107-132. https://doi.org/10.4236/ad.2023.112005

Lucotte, G., & Thomasset, T. (2024). Brass Particles on the Turin Shroud: Optical Microscopy Studies and SEM-EDX Analyses. *International Journal of Sciences, 13,* 10-32. https://doi.org/10.18483/ijsci.2812

Lucotte, G., Derouin, T., & Thomasset, T. (2016). Hematite, Biotite and Cinnabar on the Face of the Turin Shroud: Microscopy and SEM-EDX Analysis. *Open Journal of Applied Sciences, 6,* 601-625. https://doi.org/10.4236/ojapps.2016.69059

Lucotte, G., Thomasset, T., & Deroin, T. (2024). Iron-Rich Red Clays on the Turin Shroud: Optical Microscopy Studies and SEM-EDX Analyses. *Archaeological Discovery, 12,* 66-81. https://doi.org/10.4236/ad.2024.121004

Marion, A., & Lucotte, G. (2006). *Le Suaire de Turin et la Tunique d'Argenteuil*. Presses de la Renaissance (France).

Martin, J., & Pellerin, Y. (2008). *In "Du lin à la toile"*. Presses Universitaires de Rennes (France).